Global Biogeochemical Cycles®

RESEARCH ARTICLE
10.1029/2022GB007495

Key Points:

- Dissolved organic matter in high-latitude Canadian lakes increases in aromaticity northward as forests transition to shrublands
- High-latitude lakes that are hydrologically connected to the landscape have lower dissolved organic carbon (DOC) and are more allochthonous than isolated lakes
- DOC in many northern high-latitude lakes was influenced by autochthonous production and correlated weakly with absorbance

Supporting Information:

Supporting Information may be found in the online version of this article.

Correspondence to:

M. R. Kurek,
mrk19f@fsu.edu

Citation:

Kurek, M. R., Garcia-Tigreros, F., Wickland, K. P., Frey, K. E., Dornblaser, M. M., Striegl, R. G., et al. (2023). Hydrologic and landscape controls on dissolved organic matter composition across western North American Arctic lakes. *Global Biogeochemical Cycles*, *37*, e2022GB007495. https://doi.org/10.1029/2022GB007495

Received 15 JUN 2022
Accepted 20 DEC 2022

Hydrologic and Landscape Controls on Dissolved Organic Matter Composition Across Western North American Arctic Lakes

Martin R. Kurek[1,2], Fenix Garcia-Tigreros[3,4], Kimberly P. Wickland[5], Karen E. Frey[6], Mark M. Dornblaser[5], Robert G. Striegl[5], Sydney F. Niles[7], Amy M. McKenna[7,8], Pieter J. K. Aukes[9,10], Ethan D. Kyzivat[11], Chao Wang[12], Tamlin M. Pavelsky[12], Laurence C. Smith[11], Sherry L. Schiff[9], David Butman[3,4], and Robert G. M. Spencer[1,2]

[1]Department of Earth, Ocean and Atmospheric Science, Florida State University, Tallahassee, FL, USA, [2]National High Magnetic Field Laboratory Geochemistry Group, Tallahassee, FL, USA, [3]School of Environmental and Forest Sciences, University of Washington, Seattle, WA, USA, [4]Department of Civil and Environmental Engineering, University of Washington, Seattle, WA, USA, [5]United States Geological Survey, Water Resources Mission Area, Boulder, CO, USA, [6]Graduate School of Geography, Clark University, Worcester, MA, USA, [7]National High Magnetic Field Laboratory Ion Cyclotron Resonance Facility, Tallahassee, FL, USA, [8]Department of Soil & Crop Sciences, Colorado State University, Fort Collins, CO, USA, [9]Department of Earth & Environmental Studies, University of Waterloo, Waterloo, ON, Canada, [10]Geography & Environmental Studies, Wilfrid Laurier University, Waterloo, ON, Canada, [11]Department of Earth, Environmental & Planetary Sciences, Institute at Brown for Environment & Society, Brown University, Providence, RI, USA, [12]Department of Earth, Marine and Environmental Sciences, University of North Carolina, Chapel Hill, NC, USA

Abstract Northern high-latitude lakes are hotspots for cycling dissolved organic carbon (DOC) inputs from allochthonous sources to the atmosphere. However, the spatial distribution of lake dissolved organic matter (DOM) is largely unknown across Arctic-boreal regions with respect to the surrounding landscape. We expand on regional studies of northern high-latitude DOM composition by integrating DOC concentrations, optical properties, and molecular-level characterization from lakes spanning the Canadian Taiga to the Alaskan Tundra. Lakes were sampled during the summer from July to early September to capture the growing season. DOM became more optically processed and molecular-level aromaticity increased northward across the Canadian Shield to the southern Arctic and from interior Alaska to the Tundra, suggesting relatively greater DOM incorporation from allochthonous sources. Using water isotopes ($\delta^{18}O\text{-}H_2O$), we report a weak overall trend of increasing DOC and decreasing aromaticity in lakes that were hydrologically isolated from the landscape and enriched in $\delta^{18}O\text{-}H_2O$, while within-region trends were stronger and varied depending on the landscape. Finally, DOC correlated weakly with chromophoric dissolved organic matter (CDOM) across the study sites, suggesting that autochthonous and photobleached DOM were a major component of the DOC in these regions; however, some of the northernmost and wetland-dominated lakes followed pan-Arctic riverine DOC-CDOM relationships, indicating strong contributions from allochthonous inputs. As many lakes across the North American Arctic are experiencing changes in temperature and precipitation, we expect the proportions of allochthonous and autochthonous DOM to respond with aquatic optical browning with greater landscape connectivity and more internally produced DOM in hydrologically isolated lakes.

Plain Language Summary As the Arctic responds to warming, permafrost thaw, and variations in precipitation, the distribution of carbon pools within northern high-latitude lakes will also change. Specifically, the composition of dissolved organic matter (DOM) and how it is altered and moved from the landscape to the atmosphere will be highly dependent on local precipitation patterns and hydrology, but these relationships are not well constrained across large regions. We sampled over 70 individual lakes during the summer spanning various ecoregions from interior Canada to the Alaskan Tundra and characterized their dissolved organic carbon (DOC) concentrations and DOM composition using bulk and molecular-level analysis. Overall, DOM from these lakes was highly influenced by aquatic primary production but increased in the relative proportion of terrestrially derived organic matter as lake setting transitioned from forests to shrublands above the tree line. We also report a weak relationship between increasing DOC and decreasing terrestrial DOM as lakes become more hydrologically isolated across the pan-Arctic; however, regional trends were stronger within forested sampling areas and weaker in shrublands. With the hydrologic setting of many northern high-latitude lakes predicted to change in the coming decades, we expect the proportions of land- and aquatic-derived DOM to respond as well.

1. Introduction

Northern high-latitude boreal and Arctic regions, hereafter referred to as the pan-Arctic, contain large stores of carbon in soils, permafrost, and inland waters (Kling et al., 1991; McGuire et al., 2009, 2018; Schuur et al., 2015) that are highly responsive to ecosystem changes and act as potential sources of atmospheric greenhouse gasses (Miner et al., 2022; Plaza et al., 2019; Tranvik et al., 2009). In recent years, the pan-Arctic has experienced some of the highest rates of warming on Earth in addition to changing precipitation patterns, evapotranspiration, and permafrost thaw, causing some regions to become warmer and drier on average while others have become wetter over time (Bring et al., 2016; DeBeer et al., 2016; Kuhn & Butman, 2021). Additionally, the pan-Arctic has seen a shifting seasonality as winters are projected to become shorter with reduced snowfall and the onset of the summer growing season will occur earlier over time (Bintanja & Andry, 2017; Bring et al., 2016). Ongoing warming and changing precipitation patterns will continue to alter the pan-Arctic landscape resulting in rapid permafrost thaw (Miner et al., 2022; Schuur et al., 2015; Walter Anthony et al., 2018), northward expansion of shrubs and vegetation (Berner & Goetz, 2022; Liljedahl et al., 2020), and changes in water body morphology and distribution (Jones et al., 2011; Smith et al., 2005; Wickland et al., 2020). Indeed, pan-Arctic regions contain the highest abundance of freshwater lakes and the greatest relative areal lake extent in the world (Verpoorter et al., 2014), making these regions highly vulnerable to changes in climate. Lakes store, modify, and export large amounts of carbon from the landscape (Cole et al., 2007; Drake et al., 2018) and their role as a source or sink of atmospheric carbon varies with region making the pan-Arctic an important component in the global flux of mineralized aquatic carbon to CO_2 (Bogard et al., 2019; Hastie et al., 2018; Tranvik et al., 2009).

In addition to mineral carbon, aquatic carbon consists of organic forms, including dissolved organic carbon (DOC), which is an important regulator for CO_2 transfer to the atmosphere (Battin et al., 2009; Drake et al., 2018; Sobek et al., 2005; Tranvik et al., 2009) and will likely become increasingly important as the balance among stored carbon, primary production, and respiration is altered by climate change (Dornblaser & Striegl, 2015; Kling et al., 1991; Larsen et al., 2011; Vonk et al., 2015). Aquatic DOC, the commonly quantified part of dissolved organic matter (DOM) includes a diverse mixture of organic molecules from various terrestrial (allochthonous) and aquatic (autochthonous) sources, and functions as a crucial intermediary in the modern carbon cycle (Battin et al., 2009; Perdue & Ritchie, 2014). DOM from both allochthonous and autochthonous sources have unique chemical features that reveal information regarding its primary sourcing, transport, and processing history, all of which are useful indicators for how DOM compounds will function in aquatic environments on short time scales (Catalán et al., 2021; Hansen et al., 2016). For instance, bioavailable DOM is commonly sourced from fresh vegetation, aquatic producers, or recently thawed permafrost, and is responsible for aquatic energy transfer by serving as a carbon source for heterotrophs, ultimately being respired as CO_2 (Guillemette et al., 2013; Spencer et al., 2015; Vonk et al., 2015). In contrast, DOM from soils or vegetation that has undergone extensive biogeochemical processing during transport or due to optical exposure from long residence times is more resistant to biological degradation (Wickland et al., 2007) and tends to persist in aquatic systems (Kellerman et al., 2015; Koehler et al., 2012). Allochthonous DOM is highly aromatic and can attenuate light through the water column in lakes, thereby negatively impacting primary productivity and suppressing CO_2 fixation through a process known as browning (del Giorgio & Peters, 1994; Solomon et al., 2015).

Since the composition of aquatic DOM is often a mixture of both biolabile and stable compounds assimilated from many sources in varying proportions, high resolution techniques are needed in parallel with bulk measurements, such as absorbance and fluorescence spectroscopy, to delineate their different chemical features. Fourier transform-ion cyclotron resonance mass spectrometry (FT-ICR MS) has been used to resolve small differences between thousands of individual molecular formulae in various aquatic samples, providing molecular-level details of DOM composition (e.g., Kellerman et al., 2018). For instance, FT-ICR MS analysis has been useful in describing the proportion of different DOM sources across lakes (Johnston et al., 2020; Kellerman et al., 2015), identifying groups of molecular formulae that exhibit bio- and photo-lability (Kellerman et al., 2014; Mostovaya et al., 2017; Stubbins et al., 2010), and quantitatively related to their bulk molecular composition (Kellerman et al., 2018; Kurek et al., 2020; Poulin et al., 2017). As anthropogenic climate change has altered the mechanisms and rates of carbon transfer from aquatic DOM to atmospheric CO_2, ultra-high-resolution techniques will become increasingly valuable for identifying the movement and transformation of sensitive carbon pools.

Changes in temperature and precipitation across the Arctic will also affect lake morphology and shoreline extent as some lakes will become more connected to the landscape and surface runoff, while others will become more

isolated and dependent on subsurface permafrost thaw or even disappear entirely (Ala-aho et al., 2018; Anderson et al., 2013; MacDonald, Turner, et al., 2021; Walvoord et al., 2012). Several studies have also investigated the role of precipitation and local hydrology in regulating aquatic DOC concentration and DOM composition across northern high-latitude freshwaters, including interior Alaskan lakes (Johnston et al., 2020; Kurek et al., 2022), Canadian boreal lakes (Pugh et al., 2021), and Greenland lake outflows (Kellerman et al., 2020). Their findings suggest that aquatic DOM sourcing and processing vary seasonally throughout the ice-free period and that the local hydrologic setting is a primary control for the input of allochthonous DOM into these lakes. Typically, lakes that are more hydrologically connected to surface flow paths have lower DOC concentrations than isolated lakes, but relatively greater proportions of aromatic DOM. Additionally, thawing permafrost increases vertical connectivity of subsurface carbon pools to surface waters, resulting in greater inputs of rapidly consumed biolabile DOM, soil-derived aromatic compounds, and greenhouse gases (MacDonald, Tank, et al., 2021; Textor et al., 2019; Wickland et al., 2020).

Despite this growing body of work, relationships between hydrology, DOC concentration, and lake DOM composition across the pan-Arctic spanning multiple physiographic regions are currently not well understood. Previous studies were confined to individual sampling regions representing relatively homogenous landcover, climate, and permafrost extent across hydrologic and precipitation gradients, with different responses that varied by sampling region. To illustrate, several studies of northern high-latitude lakes from boreal regions in Scandinavia and Canada have reported the dominance of allochthonous DOC in these lakes and have predicted increases in external loading with projected warming (Kothawala et al., 2014; Lapierre et al., 2013; Larsen et al., 2011). In contrast, studies of Arctic lakes from northern high-latitude arid regions suggest that their DOM composition is mostly derived from autochthonous sources and that little allochthonous DOM is respired (Bogard et al., 2019; Johnston et al., 2019; Tank et al., 2009). Furthermore, as landcover spanning multiple regions has been increasingly recognized as an important factor in explaining northern high-latitude organic carbon dynamics (Stolpmann et al., 2021) it is also likely to influence differences in lake DOM composition. However, upscaling to the inter-regional level has been limited in its capacity to describe organic carbon cycling as many of these studies have only focused on lake sediments (e.g., Bell et al., 2020), or bulk DOC (e.g., Stackpoole et al., 2017; Stolpmann et al., 2021).

To address the uncertainties in DOM cycling at larger spatial scales and across hydrologic gradients, we build upon previous work by investigating lake DOC and DOM properties from the Canadian interior to the northern Alaskan coast using optical parameters, fluorescence spectroscopy, and molecular-level FT-ICR MS analysis. The objectives of this study were to describe DOC concentrations and DOM composition of northern high-latitude lakes at individual catchments and between larger physiographic regions and to assess spatial gradients of bulk- and molecular-level DOM properties across this region as related to landscape coverage and hydrology. Additionally, we investigated the relationships between hydrologic connectivity (as inferred by water isotopes), DOC concentration, and DOM composition across the pan-Arctic scale and compared them to previous intra-regional findings. Using these relationships, we sought to determine the most likely sources of DOM in these lakes and consider how the partitioning of lake DOM between allochthonous and autochthonous sources will respond to ongoing changes in hydrological patterns across northern high latitudes. This is one of the first studies to integrate DOC, bulk optical/fluorescent parameters, ultra-high resolution molecular composition, and hydrological tracers from lakes across multiple biomes in the North American Boreal-Arctic (~2,500 km). Our results highlight the importance of landscape and hydrology in dictating DOM composition between different regions and how the role of aquatic DOM may respond to changes in the pan-Arctic with respect to global carbon cycling.

2. Methods

2.1. Study Sites and Field Sampling

We collected water samples from lakes in the summer (July-September) within six different regions including the Peace-Athabasca Delta (PAD), Yellowknife, Wekweètì, Daring, Yukon Flats, and the North Slope (Figure 1; for detailed study site descriptions see Text S1 in Supporting Information S1). Samples (n = 90) covered the Western North American Arctic (WNAA) spanning a gradient from interior Canada to the northern Alaskan coast and were part of both the NASA Arctic Boreal Vulnerability Experiment domain (ABoVE; e.g., Loboda et al., 2017) and the NSF-funded Circumarctic Lakes Observation Network (CALON; e.g., Kurek et al., 2022). We also classified lakes using level II ecoregions as defined by Omernik (1995). Sampled lakes spanned five ecoregions including the Taiga Plains, Taiga Shield, Southern Arctic, Boreal Interior, Brooks Range Tundra, and

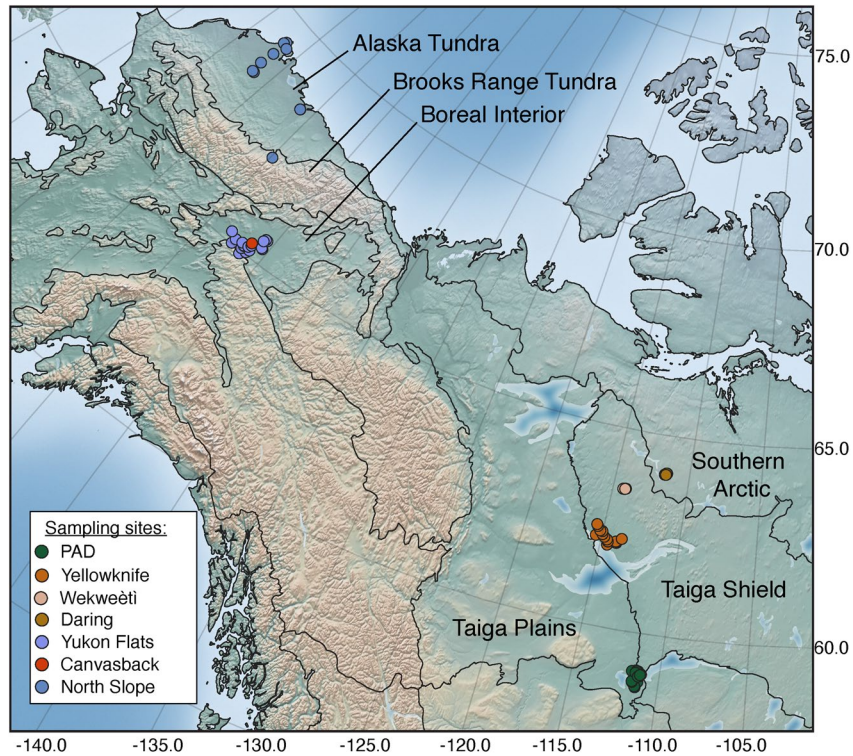

Figure 1. A map of the study sites across the Western North American Arctic (WNAA) with each sampling region colored and level II ecoregions outlined in black and labeled with text. Lakes from Johnston et al. (2020) in the Yukon Flats are also included for context (purple points). The base map is colored according to geographic relief with low relief denoted by green and high relief in tan.

Alaska Tundra (Figure 1). These ecoregions across our study sites are nearly identical to the ecozones developed by the Canadian National Ecological Framework, which are used in several past OM-centric studies (e.g., Aukes & Schiff, 2021; Bell et al., 2020). The advantage of using ecoregions to investigate lake DOM composition is that the classification scheme covers all of North America and incorporates regions based on multiple biotic and abiotic factors such as soils, landforms, geology, climate, vegetation, and hydrology (Omernik, 1995).

Surface water for DOC and DOM analysis was sampled from an open water area of each lake and filtered in the field through 0.45 μm capsule filters, or in some cases precombusted (450°C, >4 hr) Whatman GF/F filters (0.7 μm), into acid-rinsed high-density polyethylene (HDPE) bottles. Filtered samples were stored in a dark, cool (4°C) place during transport and then frozen (−20°C) until analysis. Water for isotopic analysis ($\delta^{18}O$, $\delta^{2}H$) was collected in 12 mL borosilicate vials that were filled to capacity, free of air, and stored in a dark, cool place prior to analysis. Water quality variables including Chlorophyll-a, specific conductivity (SpC) and pH were measured using YSI sensors in the field. Chlorophyll-a concentration was also measured using a Turner Designs Trilogy Fluorometer on samples from the North Slope as described previously (Kurek et al., 2022).

2.2. Oxygen and Hydrogen Water Isotopes

Stable isotopic compositions of hydrogen ($\delta^{2}H$) and oxygen ($\delta^{18}O$) in water were analyzed for a subset of lake samples in each major lake region except for the North Slope (Table S1). Water isotopes ($\delta^{18}O$ and $\delta^{2}H$) were measured at the University of Washington IsoLab laboratory and the Environmental Isotope Laboratory at the university of Waterloo using a Picarro Inc. L2130i liquid water cavity ring-down spectroscopy instrument, and following the methods as described in Schauer et al., 2016. We use the standard delta notation for $\delta^{18}O$ and $\delta^{2}H$:

$$\delta_{\text{sample}} = \left(R_{\text{sample}}/R_{\text{VSMOW}}\right) - 1$$

where R_{sample} and R_{VSMOW} are the isotopic ratios of $^{18}O/^{16}O$ and $^{2}H/^{1}H$. VSMOW is Vienna Standard Mean Ocean Water.

2.3. DOC Concentrations and Optical Analysis

Filtered water samples were acidified with HCl and analyzed for dissolved organic carbon (DOC) concentration on a Shimadzu TOC-L CPH high temperature catalytic oxidation total organic carbon analyzer (Shimadzu Corp., Kyoto, Japan). Samples were sparged with air to remove dissolved inorganic carbon and quantified using a 5-point calibration curve as described previously (e.g., Kurek et al., 2020).

Absorbance spectra were measured in a 1 cm cuvette using a Horiba Scientific Aqualog (Horiba Ltd., Kyoto, Japan) at room temperature from wavelengths of 230–800 nm. Spectral slopes were calculated at 275–295 ($S_{275\text{-}295}$) and 350–400 nm ($S_{350\text{-}400}$), and the spectral slope ratio (S_R) was calculated by dividing $S_{275\text{-}295}$ by $S_{350\text{-}400}$ (Helms et al., 2008). Chromophoric dissolved organic matter (CDOM) was determined as the Napierian absorption coefficient at 350 nm (a_{350}; m^{-1}). Specific UV absorbance at 254 nm ($SUVA_{254}$; L mg C^{-1} m^{-1}) was calculated by dividing the decadic absorption coefficient at 254 nm by the DOC concentration in mg L^{-1} (Weishaar et al., 2003). The ratio of absorbance at 250 and 365 nm (a_{250}:a_{365}) was also determined from CDOM spectra (Peuravuori & Pihlaja, 1997).

2.4. Fluorescence Spectroscopy

Excitation-Emission matrices (EEMs) were measured in a 1 cm cuvette using a Horiba Scientific Aqualog (Horiba Ltd., Kyoto, Japan) at room temperature. EEMs were collected at excitation wavelengths of 250–500 nm and emission wavelengths of 300–600 nm with 5 and 2 nm intervals, respectively, at integration times between 0.5 and 5 s. The EEMs were corrected for lamp intensity (Cory et al., 2010), inner filter effects (Kothawala et al., 2013), and normalized to Raman units (RU; Stedmon et al., 2003).

FDOM (RU) was determined as the sum of all fluorescent peak intensity maxima (nm), including peak A (Ex: 250, Em: 450), C (Ex: 350, Em: 450), M (Ex: 320, Em: 411), T (Ex: 290, Em: 349), and B (Ex: 270, Em: 304; Coble, 2007; Fellman et al., 2010). The relative proportion (%) of each fluorescent peak was reported as the intensity of each peak normalized to the sum of all peaks. The fluorescence index (FI) was calculated from the emission intensity at 470 and 520 nm at excitation 370 nm (Cory & McKnight, 2005; McKnight et al., 2001).

2.5. Solid Phase Extraction (SPE) and FT-ICR MS

Filtered water samples were acidified (pH 2) and solid phase extracted using Bond-Elut PPL columns (Agilent Technologies Inc., Santa Clara, CA) consistent with published procedures (Dittmar et al., 2008). PPL columns were soaked with methanol (>4 hr), followed by a methanol rinse, and finally rinsed with Milli-Q water at pH 2 twice. 50 µg C from each sample was isolated onto 100 mg 3 mL bed volume PPL columns, eluted with 1 mL methanol into precombusted (550°C, >4 hr) glass vials, and stored at −20°C until analysis. DOC recovery on PPL columns was measured on a subset of lakes through replicate extractions (n = 2). Methanol extracts were collected in 40 mL glass vials and the methanol was evaporated by gently drying (50°C, overnight). The organic residue was redissolved in Milli-Q water (pH 2) and shaken for several hours. DOC concentrations of the extracts were measured using methods described in Section 2.3 and reported relative to the bulk DOC of each water sample.

Methanolic extracts were analyzed on a custom-built hybrid linear ion trap 9.4-T FT-ICR MS (Oxford Corp., Oxney Mead, UK) with a 22 cm diameter bore at the National High Magnetic Field Laboratory (Tallahassee, FL) (Blakney et al., 2011; Kaiser et al., 2011). Negatively charged ions from DOM were produced via electrospray ionization (ESI) at a flow rate of 500 nL min^{-1}. Typical conditions for negative ion formation were emitter voltage, −2.4–3.0 kV; tube lens, −250 V; and heated metal capillary current, 7.2 A. Time-domain transients of 7.8 s were acquired with the Predator data station, with 100 time-domain acquisitions coadded for all experiments with an achieved resolving power of 1,600,000 at m/z 400. Peaks were internally calibrated based on several highly abundant O-containing series using a "walking calibration" (Savory et al., 2011) as described previously (e.g., Kurek et al., 2020, 2022). Reproducibility with respect to the FT-ICR MS parameters from this instrument was assessed by Zherebker et al. (2020) and was comparable to instruments from other laboratories.

Table 1
Mean Specific Conductivity (SpC), pH, Water $\delta^{18}O$, and Water $\delta^{2}H$ for Each Major Lake Region ±1σ Standard Deviation

Site	SpC (µS cm $^{-1}$)	pH	$\delta^{18}O$ (‰)	$\delta^{2}H$ (‰)
PAD	235.9 ± 125.5	8.6 ± 1.0	−11.3 ± 4.3	−115.9 ± 18.8
Yellowknife	99.5 ± 45.3	7.3 ± 0.6	−13.1 ± 1.6	−125.2 ± 7.7
Wekweètì	29.0 ± 7.1	7.2 ± 0.6	−16.8 ± 1.3	−145.0 ± 6.6
Daring	14.2 ± 1.2	6.6 ± 0.5	−17.4 ± 1.4	−145.0 ± 6.4
Canvasback Lake	892.6 ± 38.6	9.1 ± 0.3	−9.5	−104.6
North Slope	157.1 ± 81.8	7.3 ± 0.9	–	–

Note. Only one sample from Canvasback and none from the North Slope were analyzed for water isotopes.

Mass spectral peaks >6σ RMS baseline noise were exported to a peak list and processed using PetroOrg © (Corilo, 2014). Molecular formulae were assigned to ions constrained by $C_{4\text{-}45}H_{4\text{-}92}O_{1\text{-}25}N_{0\text{-}4}S_{0\text{-}2}$ and the mass measurement accuracy did not exceed 200 ppb error (e.g., Johnston et al., 2020). Molecular properties for each formula, including the modified aromaticity index (AI_{mod}) and average carbon oxidation state (C_{OX}), were calculated according to Koch and Dittmar (2006, 2016) and Mann et al. (2015), respectively. Stoichiometric ratios were calculated (H/C, O/C, N/C, S/C) as the sum of all heteroatoms divided by the sum of all carbon atoms and number-averaged across samples. Formulae were also grouped based on the percent relative abundance of their heteroatomic compositions as CHO, CHON, CHOS, and CHONS. Molecular formulae were grouped into compound classes from Šantl-Temkiv et al. (2013) including condensed aromatics (CA; $0.67 < AI_{mod}$), polyphenolics (PPh; $0.50 < AI_{mod} < 0.67$), highly-unsaturated and phenolic low O/C ($HUP_{Low\ O/C}$; $AI_{mod} < 0.50$, H/C < 1.5, O/C < 0.5), highly-unsaturated and phenolic high O/C ($HUP_{High\ O/C}$; $AI_{mod} < 0.50$, H/C < 1.5, 0.5 < O/C), and aliphatic (Ali; 1.5 < H/C), and their percent relative abundance of each class was summed. All FT-ICR MS absorption mode files are publicly available via the Open Science Framework (https://osf.io/ct3eu/) through https://doi.org/10.17605/OSF.IO/CT3EU.

2.6. Statistical Analysis

Data analysis and visualization was performed in R (R Core Team, 2020) using the ggplot2 package (Wickham, 2016). Linear regression analysis was also completed using base R and hypothesis testing was assessed at the $\alpha = 0.05$ significance level. A Principal Component Analysis (PCA) of the lakes according to their DOM properties was performed using the factoextra package in R (Kassambara & Mundt, 2017).

3. Results

3.1. Water Quality and Water Isotopes

Lakes varied in mean geochemical properties by major sampling region (Table 1). SpC was the highest at Canvasback Lake (892.6 ± 38.6 µS cm^{-1}) and lowest at lakes from the Daring (14.2 ± 1.2) and Wekweètì (29.0 ± 7.1) regions. pH was also greatest at Canvasback (9.1 ± 0.3) and the PAD (8.6 ± 1.0) and lowest at Daring (6.6 ± 0.5) with most other lakes at circumneutral. Chlorophyll-a was highest in lakes from the PAD (13.8 ± 17.5 µg L^{-1}) and lowest in lakes from the North Slope (2.1 ± 1.5 µg L^{-1}; Table S1). All lakes were enriched in heavy water isotopes relative to the global meteoric water (Figure S2 in Supporting Information S1) and spanned a range of values similar to lakes from the Yukon Flats (Table 1; Anderson et al., 2013; Johnston et al., 2020) and Greenland (Kellerman et al., 2020). Heavy water isotopes became more depleted in lakes moving north across the Canadian Shield, as expected due to fractionation from the continental effect, with the greatest variability in lakes from the PAD region. Water from Canvasback Lake was also enriched in heavy isotopes, similar to values measured previously (Johnston et al., 2020).

3.2. DOC Concentrations and DOM Optical Properties

DOC concentrations ranged from 2 to 80 mg L^{-1} across the lake regions with most below 20 mg L^{-1} (Figure 2a; Table S1). Lakes from the PAD, Yellowknife, and Canvasback Lakes had higher DOC than lakes from Daring,

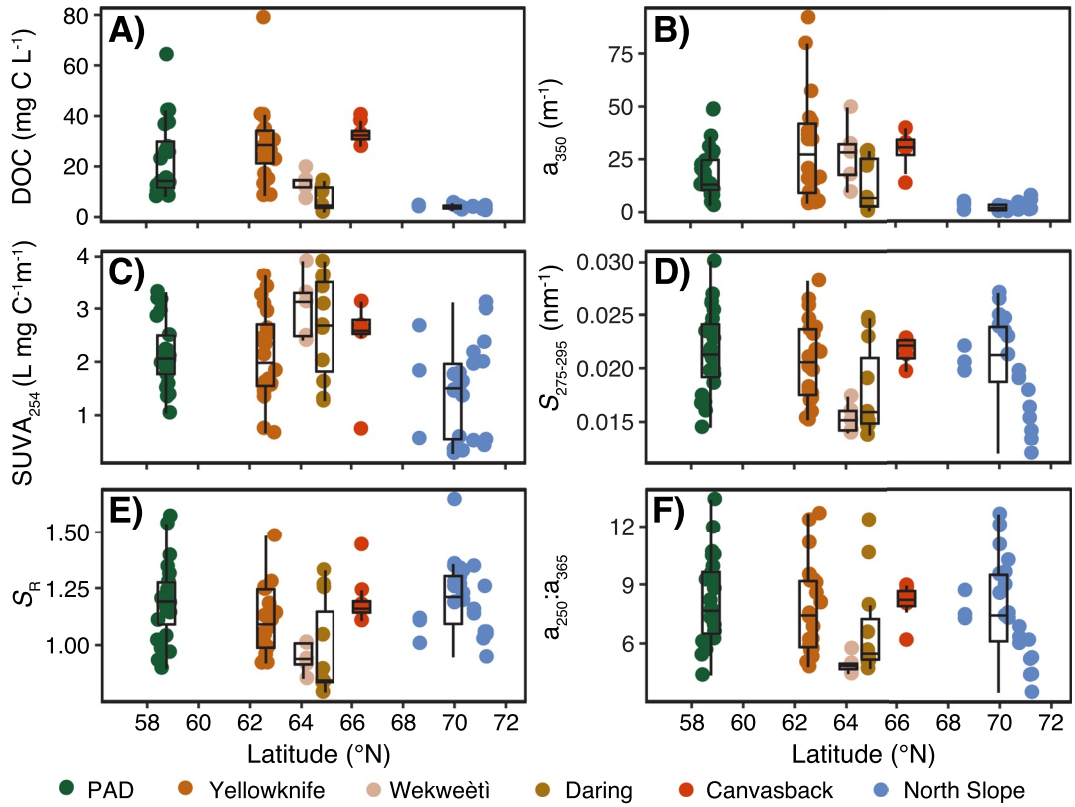

Figure 2. Boxplots of (a) dissolved organic carbon (DOC) and dissolved organic matter (DOM) optical properties from arctic lakes overlain with points ordered by latitude colored by major lake region. DOM properties include (b) chromophoric dissolved organic matter absorbance (a_{350}), (c) $SUVA_{254}$, (d) $S_{275\text{-}295}$, (e) S_R, and (f) a_{250}:a_{365}.

Wekweètì, and the North Slope (Figure 2a). The absorbance of CDOM at 350 nm (a_{350}) was highest in lakes from Yellowknife and Wekweètì, and lowest in lakes from Daring and the North Slope (Figure 2b). However, $SUVA_{254}$ values in most lakes were higher than 2.0 (Table S1) and greatest in lakes from Wekweètì, Daring, and Canvasback Lake (Figure 2c), suggesting that a greater proportion of the DOC in these lakes is aromatic (Weishaar et al., 2003). Spectral properties, including $S_{275\text{-}295}$, S_R, and a_{250}:a_{365}, followed similar trends and on average decreased in lakes from PAD to Daring and from Canvasback Lake to the coastal lakes in the North Slope region (Figures 2d–2f), suggesting that molecular size and aromaticity increased with latitude (Helms et al., 2008; Peuravuori & Pihlaja, 1997).

Most lakes regions, excluding Daring and the North Slope, had DOC concentrations comparable to those measured from the Yukon Flats (10–40 mg C L^{-1}; Johnston et al., 2020), the Mackenzie Delta (5–16 mg C L^{-1}; Tank et al., 2011), and across boreal forests (median = 15.3 mg C L^{-1}; Stolpmann et al., 2021), but concentrations were typically higher than many northern high-latitude and thawing permafrost-fed fluvial sites (0.7–27 mg C L^{-1}; Wologo et al., 2021; Johnston et al., 2021). $SUVA_{254}$ was also comparable to other lakes from the Yukon Flats (0.9–4.4 L mg C^{-1} m^{-1}; Johnston et al., 2020), Mackenzie Delta (2–4 L mg C^{-1} m^{-1}; Tank et al., 2011), and Alaskan rivers (2.0–4.5 L mg C^{-1} m^{-1}; Spencer et al., 2008; Johnston et al., 2021); however, CDOM absorbance was greater than in Alaskan rivers (mean = 16.3 m^{-1}; Johnston et al., 2021). Finally, spectral slope properties ($S_{275\text{-}295}$) were in ranges similar to lakes from the Yukon Flats (0.015–0.035 nm^{-1}; Johnston et al., 2020), but spectral slopes were generally steeper than other northern high-latitude streams (0.012–0.018 nm^{-1}; Frey et al., 2016; Johnston et al., 2021) and major Arctic rivers (0.012–0.021 nm^{-1}; Mann et al., 2016).

3.3. Fluorescent DOM Properties

Fluorescent DOM intensity (FDOM) was highest in lakes from the PAD, Yellowknife, and Canvasback Lake and lowest in lakes from the North Slope (Figure 3a; Table S1). In contrast, the fluorescence index (FI) was highest

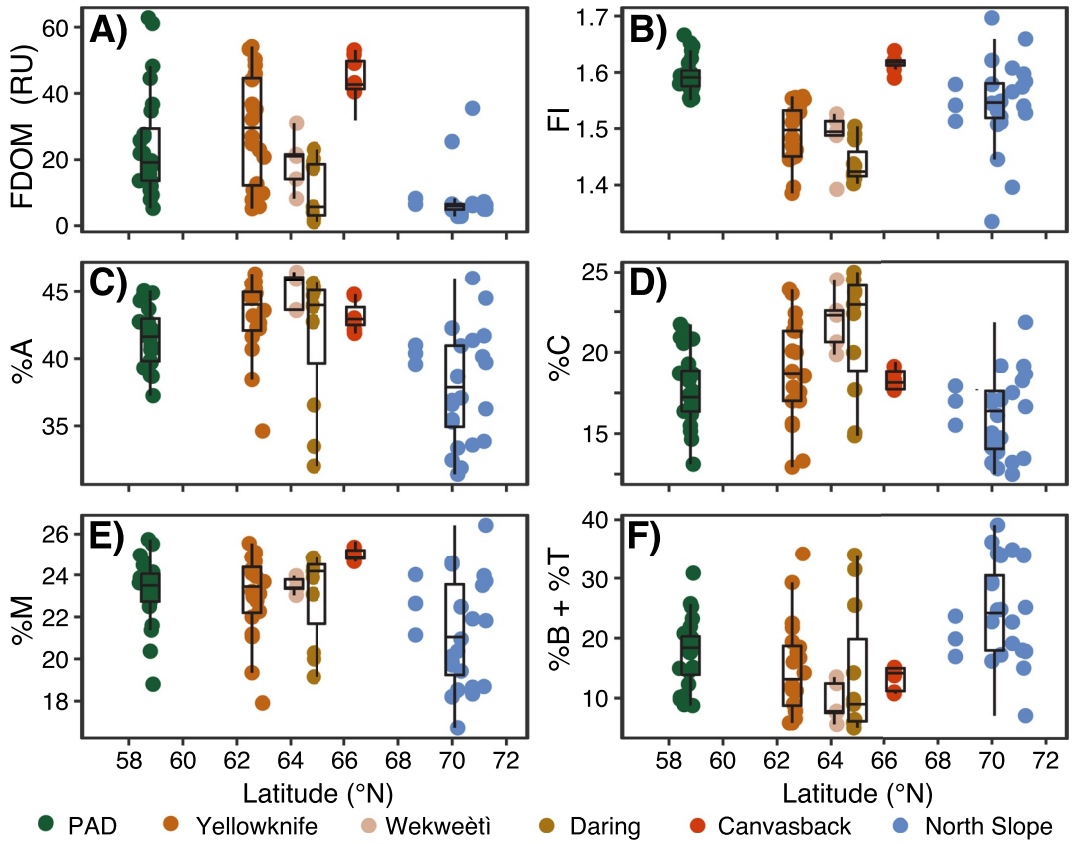

Figure 3. Boxplots of dissolved organic matter (DOM) fluorescence properties from arctic lakes overlain with points ordered by latitude colored by major lake region. DOM properties include (a) FDOM, (b) FI, (c) peak A (%), (d) peak C (%), (e) peak M (%) and (f) peaks B and T (%).

in lakes from the PAD, Canvasback, and the North Slope, ranging from 1.55 to 1.65 on average, while most lakes from Yellowknife, Wekweètì and Daring had values between 1.40 and 1.55 (Figure 3b), suggesting that they contained fewer components of fresh and autochthonous DOM (McKnight et al., 2001). Lakes generally had the highest relative fluorescent DOM contributions from peak A fluorophores, followed by peak C and peak M, and the lowest from protein-like peak B and T fluorophores (Figures 3c–3f). Lakes from the PAD and the North Slope had greater proportions of peak B and T fluorophores and a lower percentage of peak A fluorophores than lakes from Yellowknife, Wekweètì, Daring, and Canvasback (Figures 3c and 3f; Table S1).

Lake FI values across the major lake regions were similar in ranges to thawing permafrost-fed streams across the Alaska and Canada boreal region (1.50–1.70; Wologo et al., 2021), but higher than in rivers in the Yukon Basin measured during the late summer (1.39–1.43; Wickland et al., 2012), as well as from several oligotrophic lakes from the foothills of the Brook's range in interior Alaska (1.35–1.42; Cory et al., 2007). The contribution of protein-like fluorophores to FDOM from most lakes in this study was similar to lakes from the Mackenzie Delta in the summer (15%–30%; Tank et al., 2011) but greater than in streams and rivers in the Yukon Basin during summer (2.0–4.9; O'Donnell et al., 2010; Wickland et al., 2012).

3.4. DOC Recovery and FT-ICR MS Composition

DOC recoveries from SPE were measured on three lakes whose DOM composition bracketed the majority of the lakes in this study (PAD 3, NW30, Lake 10; Table S1). On average, DOC recovery was 56.5 ± 2.1% for the three lakes (PAD 3: 52.0 ± 3.4%, NW30: 55.4 ± 0.1%, Lake 10: 62.1 ± 0.5%), and was highly comparable to recoveries for extracted marine DOM (43%–62%; Dittmar et al., 2008). These recoveries suggest that the majority of DOC was retained in the PPL columns and could potentially be represented in the FT-ICR MS data. We note that SPE only isolates a subset of the bulk DOM pool and FT-ICR MS via negative electrospray preferentially ionizes

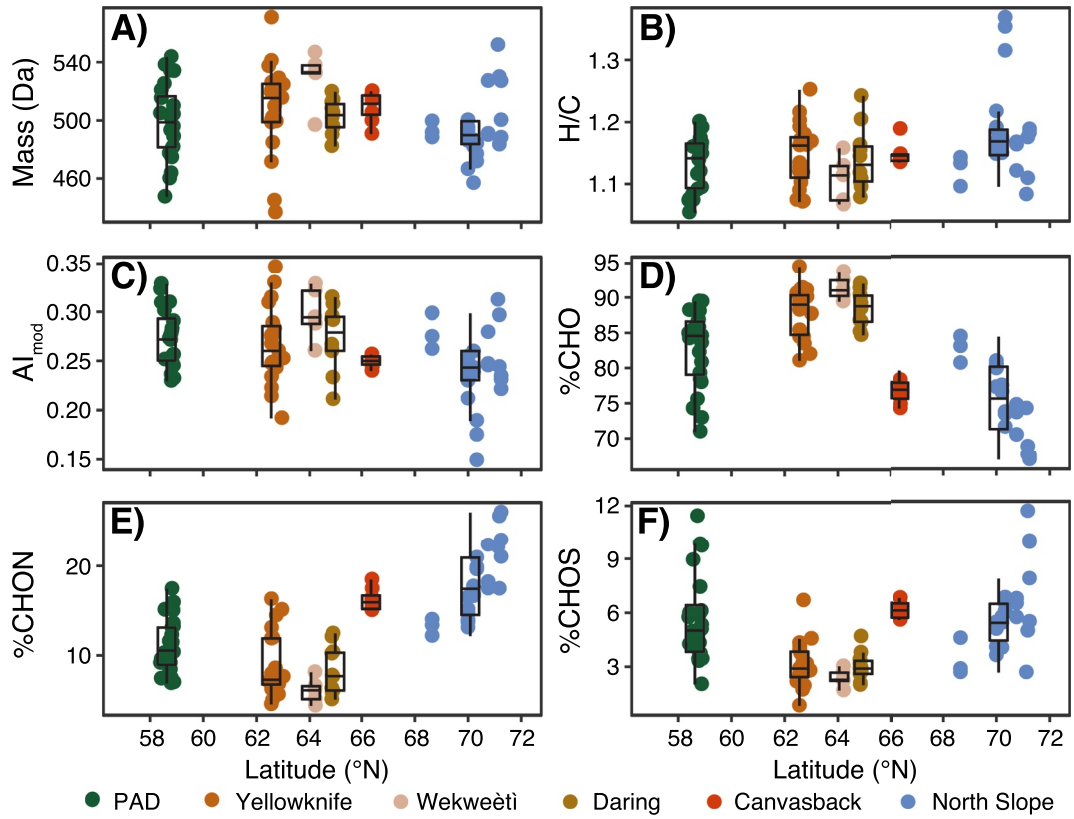

Figure 4. Boxplots of dissolved organic matter (DOM) FT-ICR MS properties from arctic lakes overlain with points ordered by latitude colored by major lake region. DOM properties include (a) Molecular weight (Mass), (b) H/C, (c) AI_{mod}, (d) CHO-containing formulae, (e) CHON-containing formulae, and (f) CHOS-containing formulae. Percentages in panels d–f represent the percent relative abundance of molecular formulae.

aromatic carboxylic acids, thereby representing only a subset of the total DOM. However, this fraction has been shown to scale quantitatively with aromaticity, carbon age, and heteroatom content (e.g., Kellerman et al., 2018; Kurek et al., 2020; Poulin et al., 2017) and is directly comparable to other molecular-level studies of Arctic DOM (e.g., Johnston et al., 2020; MacDonald, Turner, et al., 2021; MacDonald, Tank, et al., 2021; Wologo et al., 2021).

The average mass, in terms of molecular weight from FT-ICR MS spectra, was mostly in the range of 480–540 Da across the major lake regions (Figure 4a; Table S1). Average H/C ratios ranged from 1.1 to 1.2 and were slightly higher in lakes from the North Slope (Figure 4b), while average AI_{mod} was generally lower in North Slope lakes than lakes from Wekweètì and Daring (Figure 4c), suggesting that molecular formulae in the North Slope were more aliphatic and less aromatic (Koch & Dittmar, 2006, 2016). CHO-containing formulae were the most abundant of all molecular formulae and were highest in lakes from Yellowknife, Wekweètì, and Daring representing 80%–95% of the total relative abundance (Figure 4d). The percent relative abundance of CHON-containing formulae was highest in lakes from the North Slope and Canvasback Lake (15%–25%), and the percent relative abundance in CHOS-containing formulae was highest in lakes from the PAD, Canvasback Lake, and the North Slope (5%–7%) (Figures 4e and 4f). CHONS-containing formulae represented the lowest percent relative abundance of all formulae, accounting for less than 0.5% of most lake samples (Table S1).

Molecular formulae were also characterized according to compound classes based on the relative abundance of stoichiometric ratios (e.g., Šantl-Temkiv et al., 2013). $HUP_{high\ O/C}$ formulae had the highest relative abundance of all compound classes across the major lake regions (50%–70%), followed by $HUP_{low\ O/C}$ formulae (10%–40%), condensed aromatics and polyphenolics (5%–15%), and aliphatics (5%–10%; Figure 5). The relative abundance of compound classes also varied regionally. For instance, the relative abundance of aliphatic formulae was higher in lakes from the North Slope than the other lake regions (Figure 5a). $HUP_{low\ O/C}$ formulae were lower in lakes

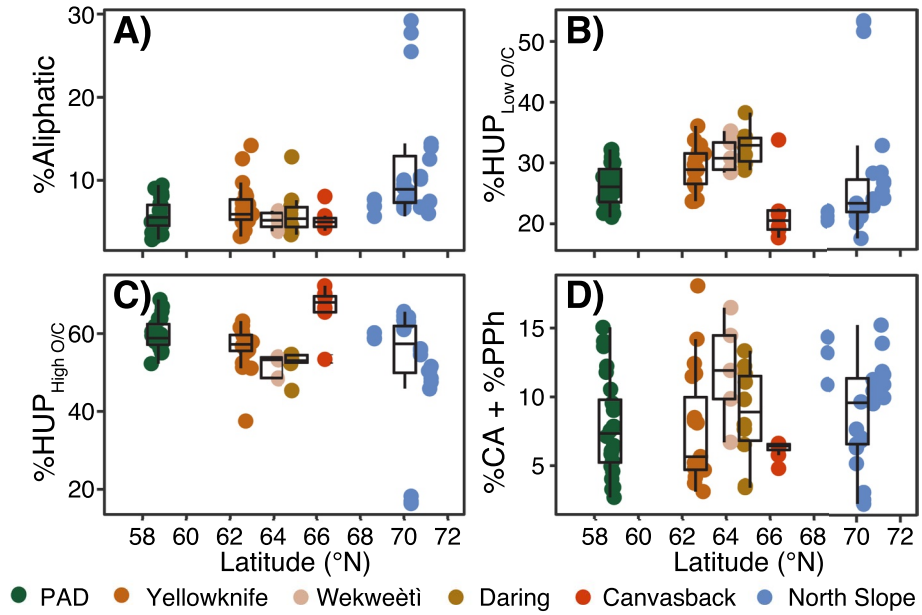

Figure 5. Boxplots of dissolved organic matter (DOM) FT-ICR MS compound classes (% relative abundance) from arctic lakes overlain with points ordered by latitude colored by major lake region. DOM compound classes include (a) Aliphatics, (b) $HUP_{Low\ O/C}$, (c) $HUP_{High\ O/C}$, and (d) Condensed aromatics (CA) + Polyphenolics (PPh).

from the North Slope, PAD, and Canvasback Lake, while $HUP_{high\ O/C}$ were higher than the other lake regions (Figures 5b and 5c).

The molecular composition of these lakes was similar to that of lakes from the Yukon Flats in terms of aromaticity (CA:<1–3%; PPh:2%–10%) and heteroatom content (CHON: 8%–16%; Johnston et al., 2020). However, DOM from lakes in this study had a higher relative abundance of aliphatics (1%–4%) and lower relative abundance of polyphenolics (5%–31%) and condensed aromatics (1%–22%) than DOM from Greenland lakes (Kellerman et al., 2020). Compared to water-extracted permafrost DOM from the western Canadian Arctic, lake DOM had higher proportions of $HUP_{high\ O/C}$ (mean = 41%) and $HUP_{low\ O/C}$ (mean = 14%) formulae and lower relative abundances of aliphatics (mean = 21%) and combined condensed aromatics with polyphenolic (mean = 24%) formulae (MacDonald, Tank, et al., 2021). In contrast, aliphatic (mean = 7%) and condensed aromatics with polyphenolic (mean = 6%) formulae were comparable to thawing permafrost-fed streams from Alaska and Canada, but lake DOM had much higher relative abundances of $HUP_{high\ O/C}$ (mean = 22%) and lower abundances of $HUP_{low\ O/C}$ (mean = 65%) formulae than the streams (Wologo et al., 2021).

3.5. Relationships Between DOM Properties and Regional Hydrology

To assess the relationships between lake DOM composition and evaporative state, DOC and DOM properties of individual lakes were examined against their water isotopes and adjusted for fractionation due to latitudinal effects (Figure 6). Adjustments were made by subtracting meteoric $\delta^{18}O$ values at each of the major lake regions (IAEA/WMO, 2021; Terzer et al., 2013) from the measured $\delta^{18}O$ values of individual lakes and reported as "$\delta^{18}O_{sample}$–$\delta^{18}O_{precipitaion}$" and hereafter referred to as "$\Delta^{18}O$." Adjusted values closer to zero are more hydrologically connected to local meteoric water sources, whereas more positive values suggest weaker hydrologic connectivity and greater evaporation. Linear regressions between lake DOM properties and adjusted water isotope values were modeled for the lakes and each lake region individually (Table 2). Regressions for the North Slope samples were not included due to unavailable data; however, we included lakes from the Yukon Flats collected in summer obtained from Johnston et al. (2020).

DOM properties were selected based on the strongest correlations reported for the Yukon Flats lakes in Johnston et al. (2020). DOC concentrations and spectral slopes ($S_{275\text{-}295}$) increased linearly across the lakes with water isotopes, but correlations with $S_{275\text{-}295}$ were only significant in the Yukon Flats, PAD, and Yellowknife, while correlations with DOC were only significant in the Yukon Flats and the PAD (Figures 6a and 6c; Table 2). In

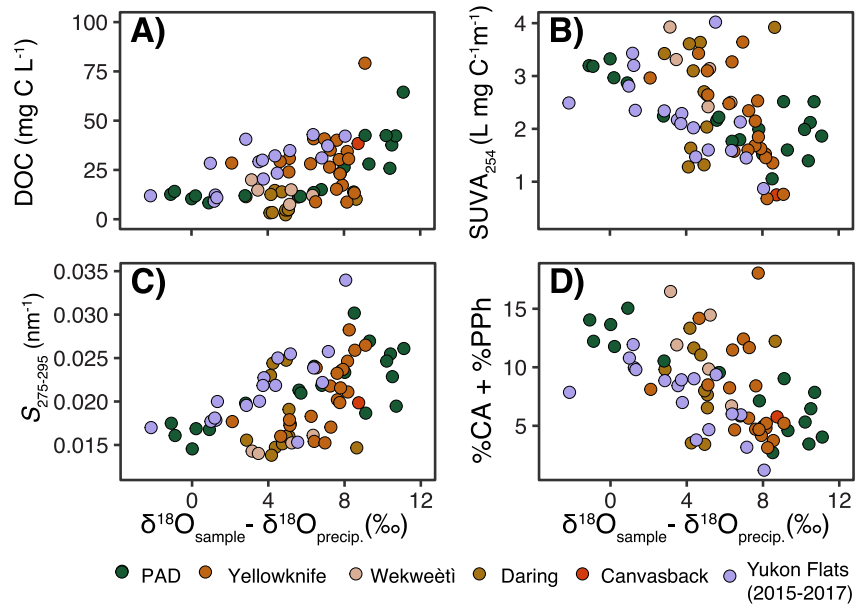

Figure 6. Scatterplots of (a) dissolved organic carbon, (b) $SUVA_{254}$, (c) $S_{275\text{-}295}$, and (d) the percent relative abundance of condensed aromatics (CA) and polyphenolics (PPh) with water $\delta^{18}O_{sample}$–$\delta^{18}O_{precipitaion}$ ($\Delta^{18}O$). Samples are colored by their major lake regions. Yukon Flats data is from Johnston et al. (2020).

contrast, $SUVA_{254}$ and the combined relative abundance of condensed aromatics and polyphenolics decreased linearly across all lakes, but correlations with $SUVA_{254}$ were only significant in the Yukon Flats, PAD, and Yellowknife, whereas correlations with polyphenolics and condensed aromatics were only significant in the Yukon Flats and the PAD (Figures 6b and 6d; Table 2). Correlations of DOM properties with water isotopes in the Wekweètì region followed the trends of all the combined lakes, but the correlations were not significant, whereas DOM properties from lakes in the Daring region did not correlate with water isotopes (Table 2).

4. Discussion

4.1. Lake DOM Composition Varies in Aromaticity and Freshness Across the Arctic

Our results complement a growing number of lake-centered organic carbon studies across the pan-Arctic (e.g., Johnston et al., 2020; Larsen et al., 2011; Stolpmann et al., 2021) and further extend our knowledge of DOM cycling by including detailed molecular composition via FT-ICR MS from all sampling locations. Individual lakes varied in DOM composition within each region, but there were two broad spatial patterns among the different regions. First, from the PAD to Daring, the lakes became more depleted in $\delta^{18}O$ and DOM was more aromatic, greater in molecular weight, lower in heteroatom content, and lower in protein-like fluorescence

Table 2
Linear Regression Coefficients (r^2) of Dissolved Organic Matter Properties With $\delta^{18}O_{sample}$–$\delta^{18}O_{precipitaion}$ ($\Delta^{18}O$) From all Samples in Each Major Lake Region

Site	DOC	$SUVA_{254}$	$S_{275\text{-}295}$	CA + PPh (%)
All (n = 73)	0.27*	0.25*	0.27*	0.28*
Yukon Flats 2015–2017 (n = 17)	0.30*	0.28*	0.50*	0.50*
PAD (n = 20)	0.54*	0.59*	0.59*	0.76*
Yellowknife (n = 20)	<0.1	0.49*	0.42*	0.12
Wekweètì (n = 5)	0.56	0.43	0.73	0.53
Daring (n = 10)	<0.1	<0.1	<0.1	<0.1

Note. Asterisks (*) indicate significance at the α = 0.05 level.

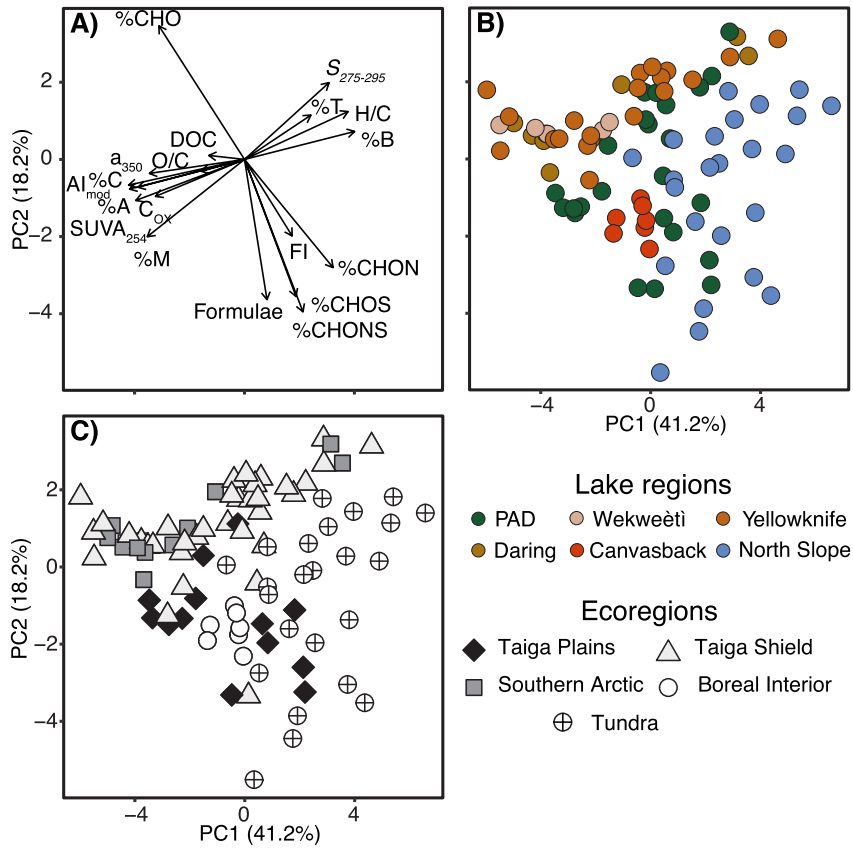

Figure 7. Principal Component Analysis biplot (PC1 vs. PC2) of dissolved organic carbon and dissolved organic matter (DOM) properties from optical, fluorescence, and FT-ICR MS analysis. (a) presents the DOM variables as vectors, (b) presents each sample as points colored by the major lake regions, and (c) presents each sample as points with shapes and shading denoting their ecoregions.

(Table 1; Figures 2–4). Second, lakes from the Alaska interior to the tundra decreased in DOC concentration and aromaticity and increased in heteroatom content as well as molecular aliphaticity (Figure 2; Figures 4 and 5). Although Canvasback Lake only represents one site within the Yukon Flats, the DOC concentration and DOM composition of this lake are highly representative of past measurements across other lakes in the Yukon Flats area spanning over 100 km (Johnston et al., 2020). However, within the tundra lakes region there were no consistent spatial trends with lakes except for higher heteroatom content and shallower spectral slope parameters in lakes closer to the coast of the Beaufort Sea (Figures 2d–2f and 4d–4f; Kurek et al., 2022). There were also no clear temporal trends within the tundra lakes during the summer sampling.

A PCA was conducted on the different lakes using DOC concentration and DOM properties to identify trends in DOM composition between the different regions (Figure 7, Table S2 in Supporting Information S1). 59.4% of the variance was explained using two components (PC1, PC2), with additional 12.6% explained with a third component (PC3; Figure S3 in Supporting Information S1). PC1 (41.2%) was strongly influenced by %C, %A, %B, $SUVA_{254}$, a_{350}, H/C, and AI_{mod}, whereas PC2 (18.2%) was driven by FI, %CHO, %CHOS, %CHON, and the number of assigned molecular formulae (Table S2 in Supporting Information S1). Thus, PC1 describes overall DOM aromaticity, where more negative values of PC1 suggest relatively greater allochthonous DOM composition and positive values suggest less. This is largely based on the inverse relationship of PC1 with variables describing molecular aromaticity (e.g., $SUVA_{254}$, AI_{mod}, %C), where more aromatic DOM likely originates from allochthonous sources (Hansen et al., 2016; Mostovaya et al., 2017). But unlike in the Yukon Flats, positive values of PC1 do not necessarily indicate a greater proportion of autochthonous DOM (Johnston et al., 2020) as many of the Tundra lakes have low productivity (Kurek et al., 2022). Next, PC2 describes DOM "freshness" and degradation extent, where positive PC2 values indicate DOM that has been degraded and negative values represent DOM that has more recently been incorporated into the waterbody. Fresh DOM typically has a higher

FI, is enriched in heteroatom-containing formulae, with a greater number-based diversity of molecular formulae that are homogenized through processing (Hansen et al., 2016; Kellerman et al., 2015; Mentges et al., 2017).

PCA revealed that the main differences between the DOM composition in northern high-latitude lakes were related to DOM sourcing and processing. Lakes from Daring, Wekweètì, and many from Yellowknife were mostly composed of allochthonous DOM (Figure 7), whereas DOM from the other regions was compositionally less allochthonous. This is also supported by the various molecular compound classes; lakes from Daring and Wekweètì had greater proportions of condensed aromatics and polyphenolics with fewer aliphatics than lakes from the PAD or Alaska (Figure 5d). Additionally, many of these properties describing PC1 (e.g., steeper spectral slopes and higher H/C ratios) may also be indicative of photobleached allochthonous DOM (Helms et al., 2008; Stubbins et al., 2010), suggesting that water residence times also vary across these lakes and may influence the composition of allochthonously sourced DOM. This is also supported by the range in $\Delta^{18}O$ between the sites as more depleted values, such as in Daring and Wekweètì, suggest shorter water residence times than enriched values, such as in the PAD or Yellowknife (Table 1). To a lesser degree, DOM from these lakes also varied in freshness. DOM from lakes in the North Slope region and in Canvasback Lake was less degraded than from Yellowknife, Wekweètì, and Daring, while lakes from the PAD were distributed along PC2 (Figure 7). Furthermore, lakes from Yellowknife, Wekweètì, and Daring had lower average proportions of aliphatic and $HUP_{high\ O/C}$ formulae than the other regions. Aliphatic and oxygenated aromatic formulae, similar in composition to $HUP_{high\ O/C}$, are likely indicators of DOM freshness as both have been correlated with higher decay rates in other boreal lakes (Mostovaya et al., 2017).

4.2. Arctic Lake DOM Composition at the Ecoregion Level

Upscaling lake DOM properties from discrete sampling sites to larger regions has been useful in delineating ecosystem processes (e.g., Aukes & Schiff, 2021; Bogard et al., 2019). For instance, Bell et al. (2020) classified the organic matter composition from Canadian lake sediments using several regional groupings and found that geological and ecological parameters were the most suitable for describing the composition while permafrost extent was the least effective, possibly due to the broad spatial resolution of the permafrost groups. In this study, analysis of lake DOM composition with permafrost extent and active layer thickness at finer resolutions (~1 km) only revealed compositional differences between Tundra lakes underlain by continuous (100%) coverage and the other sites; however, this was mostly along PC1 and overlapped with lakes underlain by sporadic coverage (10%–50%) (Figure S4a; Text S2 in Supporting Information S1). Similarly, Tundra lakes with shallow active layers (0–0.5 m) grouped separately from lakes with deeper active layers (0.5–1.5 m) but overlapped with PAD lakes that had no permafrost influence (Figure S4b in Supporting Information S1), possibly related to soil type or organic content. This suggests that permafrost extent does not sufficiently explain the variance in the lake DOM composition from this study, potentially since these lakes were sampled during late summer when the biolabile DOM signatures leached from the active layer during early summer have already been processed (Spencer et al., 2015; Vonk et al., 2015). However, ecoregion classifications have been significantly correlated with lake DOC concentration across the pan-Arctic (Stolpmann et al., 2021) and provide complementary information to the groupings of lake DOM in this study (Figure 7c).

The most apparent compositional differences were among lakes in the Alaska Tundra and those from the Southern Arctic and Taiga Shield, largely driven by DOM freshness (i.e., PC2; Figure 7c). Lakes clustering above PC2 = 0 are exclusively part of the Southern Arctic and Taiga Shield ecoregions, suggesting that their lake DOM compositions are more degraded and subject to common sourcing and processing despite their large geographic extent. However, the Southern Arctic and Taiga Shield lakes also spread along PC1, suggesting that they also encompass a gradient of aromaticity that increases northward across the Canadian Shield (Figures 2–4). This latitudinal trend covaries with forest cover and permafrost extent, where the northernmost lakes from these ecoregions are less forested and are underlain by continuous permafrost with exposed bedrock. Mean annual precipitation also decreases northward as these lakes experience less overall, but more intense periods of rainfall than boreal lakes (Ecosystem Classification Group, 2008, 2012), transporting large quantities of allochthonous DOM that have accumulated during the summer over short time periods. Allochthonous DOM sourced from soils and permafrost thaw have both been shown to leach aromatic DOM (MacDonald, Tank, et al., 2021; Textor et al., 2019), suggesting that both could be plausible sources to these lakes. Thus, DOM in the Wekweètì and Daring lakes are likely sourced from a combination of dispersed shrubland vegetation (Figure S1 in Supporting Information S1)

and active layer permafrost inputs that are transported across the bedrock via surface flow (Ecosystem Classification Group, 2012). In contrast, while the Alaska Tundra lakes are also arid, sparsely vegetated, and underlain by continuous permafrost (Figure S1 in Supporting Information S1), their DOM composition is less aromatic than Wekweètì and Daring (Figure 7). This is likely due to the coverage of barren landscape (Figure S1 in Supporting Information S1) and the low relief of the Alaska coastal plain (Hinkel et al., 2005) limiting the amount of allochthonous DOM that can be physically transported. These physical features result in lower overall lake DOC concentrations (Figure 2a) and a greater relative proportion of processed autochthonous DOM (Cory et al., 2007; Kurek et al., 2022).

Ecoregion classifications also revealed differences in DOM freshness between the PAD lakes split between the Taiga Shield and Taiga Plains (Figure 7c). The Taiga Plains lakes are significantly more isotopically depleted in $\delta^{18}O$, lower in DOC, and more aromatic than the other PAD lakes from the Taiga Shield (Table S3 in Supporting Information S1). Taiga Plains lakes were also more enriched in heteroatom-containing DOM than PAD lakes from the Taiga Shield (Figure 7c). This somewhat conflicts with findings from Johnston et al. (2020), where the most hydrologically connected lakes (i.e., most depleted $\delta^{18}O$ values) in the Yukon Flats were both more aromatic with lower heteroatom content than DOM from hydrologically connected lakes. In contrast, hydrologically connected lakes from the Taiga Plains were more aromatic than Taiga Shield lakes from the PAD, and also had greater heteroatom content. This mixed signature of allochthonous DOM and high molecular diversity suggests that DOM in Taiga Plains lakes were incorporated from both fresh vegetation and soil, possibly from wetlands and extensive littoral zones (Schiff et al., 1998). Indeed, while the PAD lakes from the Taiga Shield are surrounded by evergreen forests, the PAD lakes from the Taiga Plains were closer to deciduous forests, shrublands, and wetlands (Figure S1 in Supporting Information S1). Wetland-dominated catchments typically have high DOC and aromatic DOM from fresh, adjacent vegetation, which is rapidly consumed through microbial processing, resulting in a bulk DOM composition that appears both allochthonous and autochthonous (Kothawala et al., 2014; Lapierre & Del Giorgio, 2014). Thus, the surrounding landcover (even a relatively small extent of wetlands) around northern high-latitude lakes likely influences the overall DOC and DOM composition as well as its relationship with local hydrology (Ågren et al., 2008), especially at the regional level where DOM sources to lakes may vary across several kilometers.

4.3. Revisiting the Controls of Hydrologic Connectivity on Northern High-Latitude Lake DOM Composition

Several studies have suggested that the hydrology of northern high-latitude lakes is a primary control of DOC and DOM composition, though at varying spatial scales. For instance, across connected catchments (~50 km), DOC and aromaticity were highly sensitive to wet and dry periods in the Boreal Plains (Pugh et al., 2021). Similarly, precipitation and evaporation explained much of the variance in DOM composition and DOC across the Yukon Flats (~100 km; Johnston et al., 2020) and Western Greenland (~150 km; Kellerman et al., 2020). Our results suggest that this hydrologic control may be localized to sampling areas or ecoregions, and that allochthonously derived DOM is only a minor component of the bulk DOC across larger spatial scales within the pan-Arctic (~2,500 km). To illustrate, correlations between $\Delta^{18}O$ and DOC as well as DOM composition describing molecular size and aromaticity were much weaker compared to the correlations within individual sampling regions (Figure 6; Table 2) and those across the Yukon Flats (Johnston et al., 2020). While lakes from most sampling regions trended in the same direction (e.g., decreasing DOC and increasing aromaticity with hydrologic connectivity), lake DOM from the Daring region was invariant with respect to landscape hydrology (Table 2). This is likely due to the narrow range of depleted $\delta^{18}O$ values, low SpC (Table 1), and their allochthonous characters (i.e., greater aromaticity), suggesting that most of the sampled lakes from this region were strongly connected to the landscape with little variance. In contrast, lakes in the PAD had some of the most enriched $\delta^{18}O$ values and highest SpC, but with great variability (Table 1), reflecting how landscape processes from both the Taiga Plains and Taiga Shield, such as differences in forest cover and wetland extent, influence hydrologic connectivity (Ågren et al., 2008), especially at greater spatial scales where lake regions span multiple catchments.

Additionally, while pan-Arctic correlations between DOM aromaticity and hydrologic connectivity were significant (Table 2), correlations between hydrologic connectivity and DOC concentration as well as other DOM properties representing oxygenation (O/C, C_{OX}) and autochthony (%T, FI, and $S_{275\text{-}295}$), described by PC3, were even stronger (Table S4 in Supporting Information S1). This is illustrated by the linear regressions of principal

components (Figure 7) with $\delta^{18}O$ and $\Delta^{18}O$ (Table S4 in Supporting Information S1). Both PC1 and PC3 correlated positively with $\delta^{18}O$ and $\Delta^{18}O$; however, the correlations with water isotopes were much stronger with PC3 than with PC1 (Table S4; Figure S5 in Supporting Information S1). PC3 also correlated positively with other geochemical properties relating to local hydrology including pH ($r^2 = 0.38$, $p < 0.001$) and SpC ($r^2 = 0.40$, $p < 0.001$), while PC1 only weakly correlated with pH ($r^2 < 0.1$, $p < 0.05$) and SpC ($r^2 < 0.1$, $p < 0.05$; Table S4 in Supporting Information S1).

Taken together, this suggests that the differences between the lake DOM composition, explained by PC1 and PC3, are controlled by different aspects of local hydrology. One aspect, described by PC1, controls aromaticity where lakes that are more connected to external water sources have more allochthonous DOM that is independent of the bulk DOC concentration. The other relationship is described by PC3 where lakes that are more hydrologically disconnected with longer water residence times have more DOC and autochthonous DOM from primary production that is also subjected to biological and photochemical processing (Kellerman et al., 2014; Kothawala et al., 2014). However, unlike in the Yukon Flats where allochthonous and autochthonous composition was controlled by one axis and DOC concentration by another (Johnston et al., 2020), these two sources were decoupled from each other across the pan-Arctic with DOC concentration related mostly to autochthonous DOM. To illustrate, lakes that had higher DOC and more autochthonous DOM (PC3 > 0) spanned a whole range of aromaticity along PC1 where the least aromatic of these lakes were from the tundra and the most aromatic included the wetland-dominated lakes from the PAD (Figure S3 in Supporting Information S1). Furthermore, lakes with low aromatic DOM content (PC1 > 0) did not necessarily have greater primary production, as evidenced from the weak linear relationship between PC1 with pH and the non-significant relationship with chlorophyll-*a* (Table S4 in Supporting Information S1).

4.4. Allochthonous and Autochthonous Contributions to Northern High-Latitude Lake DOM

The fact that the DOC concentration is not a significant contributor to PC1 but rather to PC3 suggests that DOC may be more related to autochthonous DOM production and photochemical alterations than allochthonous DOM input. Consequently, allochthonous DOM may only be a minor component of the total DOC in WNAA lakes. This is evident from the weak relationship between DOC and a_{350} ($r^2 = 0.47$) across the sampled lakes compared to Arctic rivers and the high variability of lakes from each region (Figure 8). Furthermore, the slope of this relationship (0.82; Figure 8a) is shallower than slopes from previously reported riverine pan-Arctic relationships (2.25–2.47; Figure 8, dashed lines), representing terrigenous DOM in the six largest arctic rivers (Mann et al., 2016; Spencer et al., 2009, 2012). This deviation from the riverine DOC-CDOM relationship was also observed for Yukon Flats lakes sampled from 2015 to 2017 (Figure 8a, purple points); however, the overall regression for this relationship was stronger and more significant than in Johnston et al. (2020), as we only included summer samples and extended the lower DOC concentration limit by adding the tundra lakes (Figure 8a, blue points). While most lakes are scattered around the regression line, several points follow the riverine pan-Arctic regression lines, particularly from Daring and Wekweètì (Figure 8a). These lakes that follow the pan-Arctic regression have shallow spectral slopes (Figure 8b), the highest proportion of polyphenolic and condensed aromatic formulae (Figure 8c), and are the most depleted in $\delta^{18}O$ (Figure 8d), suggesting their DOM sourcing and processing is most similar to that of Arctic rivers (i.e., dominated by allochthonous inputs). In contrast, the lakes that do not follow the pan-Arctic regressions cover a continuous gradient of DOM properties where the slope of the DOC-CDOM relationship becomes shallower with less allochthonous input, ultimately approaching an endmember where the DOC-CDOM relationship is controlled by autochthonous DOM and photodegradation. Even the tundra lakes, which had similar landcover and permafrost coverage to Daring and Wekweètì (Figure S1 in Supporting Information S1), had shallower CDOM-DOC slopes (0.5–1.2) than the pan-Arctic DOC-CDOM riverine slopes (Kurek et al., 2022), further highlighting the minor contribution of allochthonous DOM to lakes in this low relief region.

Autochthonous DOM has lower CDOM absorbance, lower molecular aromaticity, and steeper spectral slopes than allochthonous leachates and lake DOM (Hansen et al., 2016; Helms et al., 2008; Johnston et al., 2019). Although autochthonous endmembers were not sampled from these sites, several studies have reported weaker DOC-CDOM relationships from autochthony. For instance, the St. Lawrence River has a shallower DOC-CDOM slope (0.275) than other North American rivers (1.65–3.38) due to most of its DOC originating from primary production in the Great Lakes (Spencer et al., 2012). Similarly, Johnston et al. (2022) reported lower CDOM

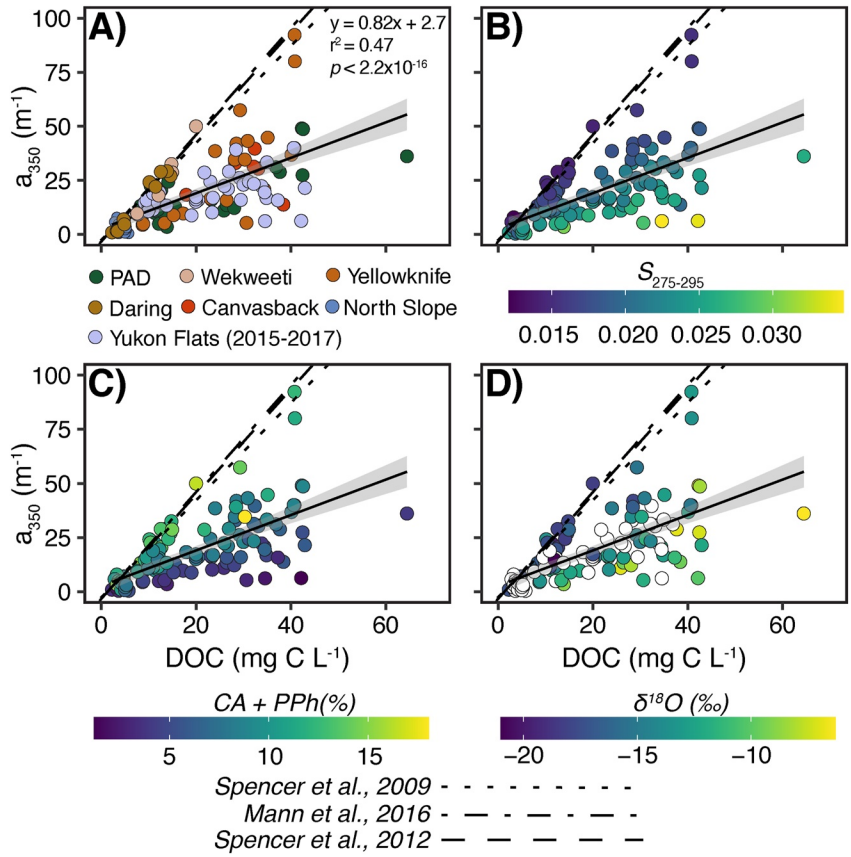

Figure 8. Linear relationships between chromophoric dissolved organic matter absorbance (a_{350}) and dissolved organic carbon. Samples are colored by (a) major lake region, (b) $S_{275\text{-}29}$, (c) percent relative abundance of condensed aromatics (CA) + polyphenolics (PPh), and (d) water $\delta^{18}O$. White points in panel d represent samples that did not have available $\delta^{18}O$ measurements. Solid black line represents the linear regression of all samples with the 95% confidence interval shaded in gray. Dashed and dotted black lines represent linear regressions from other published pan-Arctic riverine DOMs.

absorbance and shallower slopes for DOC-CDOM relationships in zooplankton leachates compared to lakes they were sampled from in North America, including Canvasback Lake. Furthermore, photobleached allochthonous DOM shares similar aliphatic signatures to autochthonous DOM (Helms et al., 2008; Stubbins et al., 2010), and often co-occurs in lakes with high productivity and long water residence time (Kothawala et al., 2014). Therefore, using CDOM absorbance to predict DOC in many northern high-latitude lakes may underestimate their true DOC concentration. Unlike in most rivers, where DOC is primarily sourced from allochthonous DOM and directly proportional to CDOM, many lakes from this study contain DOM from a mixture of sources but are more influenced by the optically inactive autochthonous endmembers and vary in their water residence times. Thus, a high proportion of autochthonous DOM makes relationships with DOC and optical parameters difficult to model in lakes and results in large variability between individual locations (e.g., Figures 2–5).

Furthermore, a greater proportion of autochthonous DOM presents unique challenges for characterizing DOM via SPE and FT-ICR MS analysis, as many of these non-aromatic formulae are not extracted in PPL and poorly ionized in negative electrospray (Gonsior et al., 2011; Li et al., 2017). Given that almost half of the DOC was not extracted through PPL (see Section 3.4), future studies of pan-Arctic lake DOM may benefit from a combination of direct sample infusion (e.g., Spencer et al., 2015) and ionization modes that target more saturated and less oxygenated formulae, such as atmospheric pressure photoionization (APPI; Kurek et al., 2020) to fully characterize their molecular composition and compare them to bulk optical metrics. Our findings expand on studies suggesting that much of the lake DOM across interior Alaska is not incorporated from allochthonous sources but rather internally produced from rapidly cycled respiration products (Bogard et al., 2019; Tank et al., 2009). However, this proportion may decrease relative to allochthonous contributions given ongoing changes in the Arctic.

4.5. The Role of DOM in a Dynamic Arctic

As temperature and precipitation patterns continue to change across the pan-Arctic (Bintanja & Andry, 2017; DeBeer et al., 2016), their effects will be reflected at the ecosystem level through their lake DOM composition. Over the past 35 years, most of the WNAA experienced higher air temperatures with many regions, such as the Alaskan Tundra and Canadian Shield, also receiving greater precipitation during the growing season. In contrast, other regions, such as Interior Alaska and the Canadian Boreal Plains, have also warmed but experienced less precipitation (DeBeer et al., 2016; Ireson et al., 2015; Kuhn & Butman, 2021). In response, most lakes across the WNAA, including the lake regions from this study except the North Slope (Figure S6 in Supporting Information S1), have declined in optical greenness, which is a strong indicator of photosynthetic pigments and primary production (Kuhn & Butman, 2021; Kuhn et al., 2020). As lake greenness declines across the WNAA, the DOC-CDOM relationship will likely strengthen, resulting in a steeper regression slope that approaches the pan-Arctic riverine relationships (i.e., one dominated by allochthonous inputs; Figure 8). Many lakes will receive a greater proportion of allochthonous DOM via surface flow paths, as has been predicted in other high-latitude lakes (e.g., Larsen et al., 2011). The input of additional allochthonous DOM will increase the bulk aromaticity of the lakes and may lead to a reduction in phototrophy via browning, shifting many lakes to net heterotrophic (del Giorgio & Peters, 1994; Solomon et al., 2015) and potentially increasing photodegradation (Lapierre et al., 2013). While microbial consumption of allochthonous DOM is often less preferential than autochthonous DOM due to its aromaticity and processing history (Guillemette et al., 2013), an expansion of wetlands, such as in the Taiga Plains PAD lakes, may deliver fresh DOM from adjacent vegetation increasing both the aromatic DOM content and biolabile DOM such as protein-like compounds, which are readily mineralized by microorganisms (Behnke et al., 2021; Lapierre & Del Giorgio, 2014). Thus, as these lakes become more connected to fresh terrigenous DOM sources, microbial communities will likely respond resulting in increased respiration, shifting of lakes to overall CO_2 sources, and changes to their benthic ecological structure (Jansson et al., 2007; Lapierre et al., 2013).

In contrast, some lakes across the WNAA are greening, although these spatial patterns are mostly restricted to the Northern Arctic and the Alaskan Tundra where the North Slope lakes were sampled (Figure S6 in Supporting Information S1; Kuhn & Butman, 2021). In this region, many coastal lakes are predicted to continue greening in the next decade, particularly those that are east of the Barrow peninsula (Lara et al., 2018). As these lakes become more productive and disconnected from the landscape, internal DOC concentrations will likely increase and aromaticity will decline, weakening the DOC-CDOM relationship as more autochthonous DOM is produced throughout the summer (Figure 8). Since this autochthonous DOM is typically more biolabile relative to allochthonous DOM (Guillemette et al., 2013), it will be rapidly consumed after the summer growing season and cycled internally, ensuring that these lakes remain net autotrophic carbon sinks (Bogard et al., 2019). However, the spatial heterogeneity of landscape cover and the variability between individual lakes highlight the difficulty of upscaling lake DOM cycling to the ecoregion level, much like the heterogeneities in terrestrial Arctic greening (Myers-Smith et al., 2020). For instance, many lakes from the western Alaskan Tundra are also predicted to experience browning (Kuhn & Butman, 2021; Lara et al., 2018) and changes to ice cover near the coast (Kurek et al., 2022), both of which will influence the extent of aromatic DOM processing. Furthermore, even though lakes from the Yukon Flats have declined in greenness, implying that aquatic productivity is decreasing (Figure S6 in Supporting Information S1), many of these lakes have been receding in surface area or infilling with rooted vegetation and becoming more disconnected from the landscape (Anderson et al., 2013). In this region, warming-induced permafrost thaw will be the dominant process for controlling DOC input and DOM composition (Dornblaser & Striegl, 2015; Walvoord et al., 2012) and will have a similar effect to wetland expansion (i.e., more aromatic and biolabile DOM); however, the proportion of biolabile DOM that will assimilate into these lakes is currently unknown as permafrost leachates are enriched in these compounds but they are rapidly consumed during thawing and transport (Spencer et al., 2015; Vonk et al., 2015).

5. Conclusion

Although this study only presents data from a relatively small fraction of the many lakes in the WNAA, it covers a large spatial transect and provides a holistic overview of many of the findings from individual catchments that capture the relationship between hydrologic connectivity and DOM composition. Lake DOC and DOM properties were in ranges similar to regional studies from other northern high-latitude lakes. However, we expand on previous findings of DOM composition from this region by reporting a northward increase in lake DOM aromaticity

across the WNAA as permafrost coverage increases and forests transition to shrublands. Additional latitudinal trends with lake DOM were absent and instead DOM composition, including aromaticity and freshness, varied by ecoregion through differences in landscape coverage and carbon sourcing. Furthermore, many of these landscape differences were related to local hydrology. Lakes that were more hydrologically connected to the landscape had lower DOC concentrations and greater aromaticity than isolated lakes, which were more processed. This agreed with several localized studies (e.g., Johnston et al., 2020; Kellerman et al., 2020); however, these relationships were weak across the pan-Arctic scale (~2,500 km) with DOM in certain lake regions unresponsive to changes in hydrology due to their extensive surface flow paths and continuous permafrost coverage (e.g., Daring). Finally, DOM in many of these lakes was influenced by autochthonous production and photodegradation as DOC concentrations were decoupled from allochthonous input and correlated weakly with optical absorbance. As the Arctic changes in the coming decades, further research is needed to evaluate how DOM composition and processing may respond to inputs of external carbon sources, such as from the landscape and permafrost thaw, as well as expansion of new flow paths, such as in wetlands and the subsurface.

Conflict of Interest

The authors declare no conflicts of interest relevant to this study.

Data Availability Statement

The authors declare that all data supporting the results of this study are archived in the Open Science Framework (https://doi.org/10.17605/OSF.IO/CT3EU).

Acknowledgments
This research was supported by the NASA ABoVE project 80NSSC19M0104 and funding from the NSF Arctic Observing Network (AON): AON-1107596 to K. E. F; and the USGS Biological Carbon Sequestration Program. Funding to SLS from the Advancing Climate Change Science in Canada program (ACCSC: ACCPJ-536045-2018); Sub-Arctic Metal Mobility Study (SAMMS), Global Water Futures, Canada Excellence Research Fund; and Discovery Grant Northern Supplement (DG-NRS), Natural Sciences and Engineering Research Council of Canada. A portion of this work was performed at the National High Magnetic Field Laboratory ICR User Facility, which is supported by the National Science Foundation Division of Chemistry and Division of Materials Research through DMR-1644779 and the State of Florida. We thank Jim Webster, Louis Farquharson, Ben Jones, and Guido Grosse for assistance with summer field sampling in the North Slope. We thank Richard Elgood, Roy Judas, Michael English, Mackenzie Schultz, Jeremy Leathers as well as the Wek'èezhìi Land & Water Board for their support at Yellowknife, Wekweètì and Daring Lake sites. We thank Ryan Hutchins for his insight on the manuscript and Amy Holt for her helpful comments and R code. We thank Parks Canada and Robert and Barbara Grandjambe for assistance with field sampling in the PAD. We also thank the Tłı̨chǫ First Nation communities of Wekweètì and Daring as well as the Dene First Nation of Yellowknife. Any use of trade, firm, or product names is for descriptive purposes only and does not imply endorsement by the U.S. Government.

References

Ågren, A., Buffam, I., Berggren, M., Bishop, K., Jansson, M., & Laudon, H. (2008). Dissolved organic carbon characteristics in boreal streams in a forest-wetland gradient during the transition between winter and summer. *Journal of Geophysical Research*, *113*(G3), G03031. https://doi.org/10.1029/2007jg000674

Ala-Aho, P., Soulsby, C., Pokrovsky, O. S., Kirpotin, S. N., Karlsson, J., Serikova, S., et al. (2018). Using stable isotopes to assess surface water source dynamics and hydrological connectivity in a high-latitude wetland and permafrost influenced landscape. *Journal of Hydrology*, *556*, 279–293. https://doi.org/10.1016/j.jhydrol.2017.11.024

Anderson, L., Birks, J., Rover, J., & Guldager, N. (2013). Controls on recent Alaskan lake changes identified from water isotopes and remote sensing. *Geophysical Research Letters*, *40*(13), 3413–3418. https://doi.org/10.1002/grl.50672

Aukes, P. J., & Schiff, S. L. (2021). Composition Wheels: Visualizing dissolved organic matter using common composition metrics across a variety of Canadian ecozones. *PLoS One*, *16*(7), e0253972. https://doi.org/10.1371/journal.pone.0253972

Battin, T. J., Luyssaert, S., Kaplan, L. A., Aufdenkampe, A. K., Richter, A., & Tranvik, L. J. (2009). The boundless carbon cycle. *Nature Geoscience*, *2*(9), 598–600. https://doi.org/10.1038/ngeo618

Behnke, M. I., McClelland, J. W., Tank, S. E., Kellerman, A. M., Holmes, R. M., Haghipour, N., et al. (2021). Pan-Arctic riverine dissolved organic matter: Synchronous molecular stability, shifting sources and subsidies. *Global Biogeochemical Cycles*, *35*(4), e2020GB006871. https://doi.org/10.1029/2020gb006871

Bell, M. A., Overy, D. P., & Blais, J. M. (2020). A continental scale spatial investigation of lake sediment organic compositions using sedimentomics. *Science of the Total Environment*, *719*, 137746. https://doi.org/10.1016/j.scitotenv.2020.137746

Berner, L. T., & Goetz, S. J. (2022). Satellite observations document trends consistent with a boreal forest biome shift. *Global Change Biology*, *28*(10), 3275–3292. https://doi.org/10.1111/gcb.16121

Bintanja, R., & Andry, O. (2017). Towards a rain-dominated Arctic. *Nature Climate Change*, *7*(4), 263–267. https://doi.org/10.1038/nclimate3240

Blakney, G. T., Hendrickson, C. L., & Marshall, A. G. (2011). Predator data station: A fast data acquisition system for advanced FT-ICR MS experiments. *International Journal of Mass Spectrometry*, *306*(2–3), 246–252. https://doi.org/10.1016/j.ijms.2011.03.009

Bogard, M. J., Kuhn, C. D., Johnston, S. E., Striegl, R. G., Holtgrieve, G. W., Dornblaser, M. M., et al. (2019). Negligible cycling of terrestrial carbon in manyf lakes of the arid circumpolar landscape. *Nature Geoscience*, *12*(3), 180–185. https://doi.org/10.1038/s41561-019-0299-5

Bring, A., Fedorova, I., Dibike, Y., Hinzman, L., Mård, J., Mernild, S. H., et al. (2016). Arctic terrestrial hydrology: A synthesis of processes, regional effects, and research challenges. *Journal of Geophysical Research: Biogeosciences*, *121*(3), 621–649. https://doi.org/10.1002/2015jg003131

Catalán, N., Pastor, A., Borrego, C. M., Casas-Ruiz, J. P., Hawkes, J. A., Gutiérrez, C., et al. (2021). The relevance of environment vs. composition on dissolved organic matter degradation in freshwaters. *Limnology & Oceanography*, *66*(2), 306–320. https://doi.org/10.1002/lno.11606

Coble, P. G. (2007). Marine optical biogeochemistry: The chemistry of ocean color. *Chemical Reviews*, *107*(2), 402–418. https://doi.org/10.1021/cr050350

Cole, J. J., Prairie, Y. T., Caraco, N. F., McDowell, W. H., Tranvik, L. J., Striegl, R. G., et al. (2007). Plumbing the global carbon cycle: Integrating inland waters into the terrestrial carbon budget. *Ecosystems*, *10*(1), 172–185. https://doi.org/10.1007/s10021-006-9013-8

Corilo, Y. E. (2014). *PetroOrg software*. Florida State University; All Rights reserved. Retrieved from http://www.petroorg.com

Cory, R. M., & McKnight, D. M. (2005). Fluorescence spectroscopy reveals ubiquitous presence of oxidized and reduced quinones in dissolved organic matter. *Environmental Science & Technology*, *39*(21), 8142–8149. https://doi.org/10.1021/es0506962

Cory, R. M., McKnight, D. M., Chin, Y. P., Miller, P., & Jaros, C. L. (2007). Chemical characteristics of fulvic acids from Arctic surface waters: Microbial contributions and photochemical transformations. *Journal of Geophysical Research*, *112*(G4), G04S51. https://doi.org/10.1029/2006jg000343

Cory, R. M., Miller, M. P., McKnight, D. M., Guerard, J. J., & Miller, P. L. (2010). Effect of instrument-specific response on the analysis of fulvic acid fluorescence spectra. *Limnology and Oceanography: Methods*, *8*(2), 67–78. https://doi.org/10.4319/lom.2010.8.67

DeBeer, C. M., Wheater, H. S., Carey, S. K., & Chun, K. P. (2016). Recent climatic, cryospheric, and hydrological changes over the interior of western Canada: A review and synthesis. *Hydrology and Earth System Sciences*, *20*(4), 1573–1598. https://doi.org/10.5194/hess-20-1573-2016

del Giorgio, P. A., & Peters, R. H. (1994). Patterns in planktonic P: R ratios in lakes: Influence of Lake Trophy and dissolved organic carbon. *Limnology & Oceanography*, *39*(4), 772–787. https://doi.org/10.4319/lo.1994.39.4.0772

Dittmar, T., Koch, B., Hertkorn, N., & Kattner, G. (2008). A simple and efficient method for the solid-phase extraction of dissolved organic matter (SPE-DOM) from seawater. *Limnology and Oceanography: Methods*, *6*(6), 230–235. https://doi.org/10.4319/lom.2008.6.230

Dornblaser, M. M., & Striegl, R. G. (2015). Switching predominance of organic versus inorganic carbon exports from an intermediate-size subarctic watershed. *Geophysical Research Letters*, *42*(2), 386–394. https://doi.org/10.1002/2014gl062349

Drake, T. W., Raymond, P. A., & Spencer, R. G. (2018). Terrestrial carbon inputs to inland waters: A current synthesis of estimates and uncertainty. *Limnology and Oceanography Letters*, *3*(3), 132–142. https://doi.org/10.1002/lol2.10055

Ecosystem Classification Group. (2008). *Ecological regions of the northwest Territories—Taiga Shield*. Department of Environment and Natural Resources, Government of the Northwest Territories.

Ecosystem Classification Group. (2012). *Ecological regions of the northwest Territories—southern Arctic*. Department of Environment and Natural Resources, Government of the Northwest Territories.

Fellman, J. B., Hood, E., & Spencer, R. G. (2010). Fluorescence spectroscopy opens new windows into dissolved organic matter dynamics in freshwater ecosystems: A review. *Limnology & Oceanography*, *55*(6), 2452–2462. https://doi.org/10.4319/lo.2010.55.6.2452

Frey, K. E., Sobczak, W. V., Mann, P. J., & Holmes, R. M. (2016). Optical properties and bioavailability of dissolved organic matter along a flow-path continuum from soil pore waters to the Kolyma River mainstem, East Siberia. *Biogeosciences*, *13*(8), 2279–2290. https://doi.org/10.5194/bg-13-2279-2016

Gonsior, M., Peake, B. M., Cooper, W. T., Podgorski, D. C., D'Andrilli, J., Dittmar, T., & Cooper, W. J. (2011). Characterization of dissolved organic matter across the Subtropical Convergence off the South Island, New Zealand. *Marine Chemistry*, *123*(1–4), 99–110. https://doi.org/10.1016/j.marchem.2010.10.004

Guillemette, F., McCallister, S. L., & del Giorgio, P. A. (2013). Differentiating the degradation dynamics of algal and terrestrial carbon within complex natural dissolved organic carbon in temperate lakes. *Journal of Geophysical Research: Biogeosciences*, *118*(3), 963–973. https://doi.org/10.1002/jgrg.20077

Hansen, A. M., Kraus, T. E., Pellerin, B. A., Fleck, J. A., Downing, B. D., & Bergamaschi, B. A. (2016). Optical properties of dissolved organic matter (DOM): Effects of biological and photolytic degradation. *Limnology & Oceanography*, *61*(3), 1015–1032. https://doi.org/10.1002/lno.10270

Hastie, A., Lauerwald, R., Weyhenmeyer, G., Sobek, S., Verpoorter, C., & Regnier, P. (2018). CO 2 evasion from boreal lakes: Revised estimate, drivers of spatial variability, and future projections. *Global Change Biology*, *24*(2), 711–728. https://doi.org/10.1111/gcb.13902

Helms, J. R., Stubbins, A., Ritchie, J. D., Minor, E. C., Kieber, D. J., & Mopper, K. (2008). Absorption spectral slopes and slope ratios as indicators of molecular weight, source, and photobleaching of chromophoric dissolved organic matter. *Limnology & Oceanography*, *53*(3), 955–969. https://doi.org/10.4319/lo.2008.53.3.0955

Hinkel, K. M., Frohn, R. C., Nelson, F. E., Eisner, W. R., & Beck, R. A. (2005). Morphometric and spatial analysis of thaw lakes and drained thaw lake basins in the western Arctic Coastal Plain, Alaska. *Permafrost and Periglacial Processes*, *16*(4), 327–341. https://doi.org/10.1002/ppp.532

IAEA/WMO. (2021). Global network of isotopes in precipitation. In *The GNIP database*. Retrieved from https://nucleus.iaea.org/wiser

Ireson, A. M., Barr, A. G., Johnstone, J. F., Mamet, S. D., Van der Kamp, G., Whitfield, C. J., et al. (2015). The changing water cycle: The boreal plains ecozone of Western Canada. *Wiley Interdisciplinary Reviews: Water*, *2*(5), 505–521. https://doi.org/10.1002/wat2.1098

Jansson, M., Persson, L., De Roos, A. M., Jones, R. I., & Tranvik, L. J. (2007). Terrestrial carbon and intraspecific size-variation shape lake ecosystems. *Trends in Ecology & Evolution*, *22*(6), 316–322. https://doi.org/10.1016/j.tree.2007.02.015

Johnston, S. E., Bogard, M. J., Rogers, J. A., Butman, D., Striegl, R. G., Dornblaser, M., & Spencer, R. G. (2019). Constraining dissolved organic matter sources and temporal variability in a model sub-Arctic lake. *Biogeochemistry*, *146*(3), 271–292. https://doi.org/10.1007/s10533-019-00619-9

Johnston, S. E., Carey, J. C., Kellerman, A., Podgorski, D. C., Gewirtzman, J., & Spencer, R. G. (2021). Controls on riverine dissolved organic matter composition across an Arctic-Boreal latitudinal gradient. *Journal of Geophysical Research: Biogeosciences*, *126*(9), e2020JG005988. https://doi.org/10.1029/2020jg005988

Johnston, S. E., Finlay, K., Spencer, R. G., Butman, D. E., Metz, M., Striegl, R., & Bogard, M. J. (2022). Zooplankton release complex dissolved organic matter to aquatic environments. *Biogeochemistry*, *157*(3), 313–325. https://doi.org/10.1007/s10533-021-00876-7

Johnston, S. E., Striegl, R. G., Bogard, M. J., Dornblaser, M. M., Butman, D. E., Kellerman, A. M., et al. (2020). Hydrologic connectivity determines dissolved organic matter biogeochemistry in northern high-latitude lakes. *Limnology & Oceanography*, *65*(8), 1764–1780. https://doi.org/10.1002/lno.11417

Jones, B. M., Grosse, G. D. A. C., Arp, C. D., Jones, M. C., Anthony, K. W., & Romanovsky, V. E. (2011). Modern thermokarst lake dynamics in the continuous permafrost zone, northern Seward Peninsula, Alaska. *Journal of Geophysical Research*, *116*(G2), G00M03. https://doi.org/10.1029/2011jg001666

Kaiser, N. K., Quinn, J. P., Blakney, G. T., Hendrickson, C. L., & Marshall, A. G. (2011). A novel 9.4 Tesla FTICR mass spectrometer with improved sensitivity, mass resolution, and mass range. *Journal of the American Society for Mass Spectrometry*, *22*(8), 1343–1351. https://doi.org/10.1007/s13361-011-0141-9

Kassambara, A., & Mundt, F. (2017). Factoextra: Extract and visualize the results of multivariate data analyses. *R Package Version*, *1*(4), 337–354.

Kellerman, A. M., Dittmar, T., Kothawala, D. N., & Tranvik, L. J. (2014). Chemodiversity of dissolved organic matter in lakes driven by climate and hydrology. *Nature Communications*, *5*(1), 1–8. https://doi.org/10.1038/ncomms4804

Kellerman, A. M., Guillemette, F., Podgorski, D. C., Aiken, G. R., Butler, K. D., & Spencer, R. G. (2018). Unifying concepts linking dissolved organic matter composition to persistence in aquatic ecosystems. *Environmental Science & Technology*, *52*(5), 2538–2548. https://doi.org/10.1021/acs.est.7b05513

Kellerman, A. M., Hawkings, J. R., Wadham, J. L., Kohler, T. J., Stibal, M., Grater, E., et al. (2020). Glacier outflow dissolved organic matter as a window into seasonally changing carbon sources: Leverett Glacier, Greenland. *Journal of Geophysical Research: Biogeosciences*, *125*(4), e2019JG005161. https://doi.org/10.1029/2019jg005161

Kellerman, A. M., Kothawala, D. N., Dittmar, T., & Tranvik, L. J. (2015). Persistence of dissolved organic matter in lakes related to its molecular characteristics. *Nature Geoscience*, *8*(6), 454–457. https://doi.org/10.1038/ngeo2440

Kling, G. W., Kipphut, G. W., & Miller, M. C. (1991). Arctic lakes and streams as gas conduits to the atmosphere: Implications for tundra carbon budgets. *Science*, *251*(4991), 298–301. https://doi.org/10.1126/science.251.4991.298
Koch, B. P., & Dittmar, T. (2006). From mass to structure: An aromaticity index for high-resolution mass data of natural organic matter. *Rapid Communications in Mass Spectrometry*, *20*(5), 926–932. https://doi.org/10.1002/rcm.2386
Koch, B. P., & Dittmar, T. (2016). From mass to structure: An aromaticity index for high-resolution mass data of natural organic matter. *Rapid Communications in Mass Spectrometry*, *30*(5), 250–932. https://doi.org/10.1002/rcm.2386
Koehler, B., Von Wachenfeldt, E., Kothawala, D., & Tranvik, L. J. (2012). Reactivity continuum of dissolved organic carbon decomposition in lake water. *Journal of Geophysical Research*, *117*(G1), G01024. https://doi.org/10.1029/2011jg001793
Kothawala, D. N., Murphy, K. R., Stedmon, C. A., Weyhenmeyer, G. A., & Tranvik, L. J. (2013). Inner filter correction of dissolved organic matter fluorescence. *Limnology and Oceanography: Methods*, *11*(12), 616–630. https://doi.org/10.4319/lom.2013.11.616
Kothawala, D. N., Stedmon, C. A., Müller, R. A., Weyhenmeyer, G. A., Köhler, S. J., & Tranvik, L. J. (2014). Controls of dissolved organic matter quality: Evidence from a large-scale boreal lake survey. *Global Change Biology*, *20*(4), 1101–1114. https://doi.org/10.1111/gcb.12488
Kuhn, C., Bogard, M., Johnston, S. E., John, A., Vermote, E., Spencer, R., et al. (2020). Satellite and airborne remote sensing of gross primary productivity in boreal Alaskan lakes. *Environmental Research Letters*, *15*(10), 105001. https://doi.org/10.1088/1748-9326/aba46f
Kuhn, C., & Butman, D. (2021). Declining greenness in Arctic-boreal lakes. *Proceedings of the National Academy of Sciences of the United States of America*, *118*(15). https://doi.org/10.1073/pnas.2021219118
Kurek, M. R., Frey, K. E., Guillemette, F., Podgorski, D. C., Townsend-Small, A., Arp, C. D., et al. (2022). Trapped under ice: Spatial and seasonal dynamics of dissolved organic matter composition in tundra lakes. *Journal of Geophysical Research: Biogeosciences*, *127*(4), e2021JG006578. https://doi.org/10.1029/2021jg006578
Kurek, M. R., Poulin, B. A., McKenna, A. M., & Spencer, R. G. (2020). Deciphering dissolved organic matter: Ionization, dopant, and fragmentation insights via Fourier transform-ion cyclotron resonance mass spectrometry. *Environmental Science & Technology*, *54*(24), 16249–16259. https://doi.org/10.1021/acs.est.0c05206
Lapierre, J. F., & Del Giorgio, P. A. (2014). Partial coupling and differential regulation of biologically and photochemically labile dissolved organic carbon across boreal aquatic networks. *Biogeosciences*, *11*(20), 5969–5985. https://doi.org/10.5194/bg-11-5969-2014
Lapierre, J. F., Guillemette, F., Berggren, M., & Del Giorgio, P. A. (2013). Increases in terrestrially derived carbon stimulate organic carbon processing and CO_2 emissions in boreal aquatic ecosystems. *Nature Communications*, *4*(1), 1–7. https://doi.org/10.1038/ncomms3972
Lara, M. J., Nitze, I., Grosse, G., Martin, P., & McGuire, A. D. (2018). Reduced arctic tundra productivity linked with landform and climate change interactions. *Scientific Reports*, *8*(1), 1–10. https://doi.org/10.1038/s41598-018-20692-8
Larsen, S., Andersen, T. O. M., & Hessen, D. O. (2011). Climate change predicted to cause severe increase of organic carbon in lakes. *Global Change Biology*, *17*(2), 1186–1192. https://doi.org/10.1111/j.1365-2486.2010.02257.x
Li, Y., Harir, M., Uhl, J., Kanawati, B., Lucio, M., Smirnov, K. S., et al. (2017). How representative are dissolved organic matter (DOM) extracts? A comprehensive study of sorbent selectivity for DOM isolation. *Water Research*, *116*, 316–323. https://doi.org/10.1016/j.watres.2017.03.038
Liljedahl, A. K., Timling, I., Frost, G. V., & Daanen, R. P. (2020). Arctic riparian shrub expansion indicates a shift from streams gaining water to those that lose flow. *Communications Earth & Environment*, *1*(1), 1–9. https://doi.org/10.1038/s43247-020-00050-1
Loboda, T. V., Hoy, E., & Carroll, M. L. (2017). *ABoVE: Study domain and standard reference grids*. ORNL DAAC.
MacDonald, E. N., Tank, S. E., Kokelj, S. V., Froese, D. G., & Hutchins, R. H. (2021). Permafrost-derived dissolved organic matter composition varies across permafrost end-members in the western Canadian Arctic. *Environmental Research Letters*, *16*(2), 024036. https://doi.org/10.1088/1748-9326/abd971
MacDonald, L. A., Turner, K. W., McDonald, I., Kay, M. L., Hall, R. I., & Wolfe, B. B. (2021). Isotopic evidence of increasing water abundance and lake hydrological change in old crow flats, Yukon, Canada. *Environmental Research Letters*, *16*(12), 124024. https://doi.org/10.1088/1748-9326/ac3533
Mann, B. F., Chen, H., Herndon, E. M., Chu, R. K., Tolic, N., Portier, E. F., et al. (2015). Indexing permafrost soil organic matter degradation using high-resolution mass spectrometry. *PLoS One*, *10*(6), e0130557. https://doi.org/10.1371/journal.pone.0130557
Mann, P. J., Spencer, R. G., Hernes, P. J., Six, J., Aiken, G. R., Tank, S. E., et al. (2016). Pan-Arctic trends in terrestrial dissolved organic matter from optical measurements. *Frontiers of Earth Science*, *4*, 25. https://doi.org/10.3389/feart.2016.00025
McGuire, A. D., Anderson, L. G., Christensen, T. R., Dallimore, S., Guo, L., Hayes, D. J., et al. (2009). Sensitivity of the carbon cycle in the Arctic to climate change. *Ecological Monographs*, *79*(4), 523–555. https://doi.org/10.1890/08-2025.1
McGuire, A. D., Lawrence, D. M., Koven, C., Clein, J. S., Burke, E., Chen, G., et al. (2018). Dependence of the evolution of carbon dynamics in the northern permafrost region on the trajectory of climate change. *Proceedings of the National Academy of Sciences of the United States of America*, *115*(15), 3882–3887. https://doi.org/10.1073/pnas.1719903115
McKnight, D. M., Boyer, E. W., Westerhoff, P. K., Doran, P. T., Kulbe, T., & Andersen, D. T. (2001). Spectrofluorometric characterization of dissolved organic matter for indication of precursor organic material and aromaticity. *Limnology & Oceanography*, *46*(1), 38–48. https://doi.org/10.4319/lo.2001.46.1.0038
Mentges, A., Feenders, C., Seibt, M., Blasius, B., & Dittmar, T. (2017). Functional molecular diversity of marine dissolved organic matter is reduced during degradation. *Frontiers in Marine Science*, *4*, 194. https://doi.org/10.3389/fmars.2017.00194
Miner, K. R., Turetsky, M. R., Malina, E., Bartsch, A., Tamminen, J., McGuire, A. D., et al. (2022). Permafrost carbon emissions in a changing Arctic. *Nature Reviews Earth & Environment*, *3*(1), 55–67. https://doi.org/10.1038/s43017-021-00230-3
Mostovaya, A., Hawkes, J. A., Dittmar, T., & Tranvik, L. J. (2017). Molecular determinants of dissolved organic matter reactivity in lake water. *Frontiers of Earth Science*, *5*, 106. https://doi.org/10.3389/feart.2017.00106
Myers-Smith, I. H., Kerby, J. T., Phoenix, G. K., Bjerke, J. W., Epstein, H. E., Assmann, J. J., et al. (2020). Complexity revealed in the greening of the Arctic. *Nature Climate Change*, *10*(2), 106–117. https://doi.org/10.1038/s41558-019-0688-1
O'Donnell, J. A., Aiken, G. R., Kane, E. S., & Jones, J. B. (2010). Source water controls on the character and origin of dissolved organic matter in streams of the Yukon River basin, Alaska. *Journal of Geophysical Research*, *115*(G3), G03025. https://doi.org/10.1029/2009jg001153
Omernik, J. M. (1995). Ecoregions: A spatial framework for environmental management. *Biological Assessment and Criteria: Tools for Water Resource Planning and Decision Making*, *49*, 62.
Perdue, E. M., & Ritchie, J. D. (2014). Dissolved organic matter in freshwaters. *Treatise on Geochemistry*, *7*, 237–272. https://doi.org/10.1016/b978-0-08-095975-7.00509-x
Peuravuori, J., & Pihlaja, K. (1997). Molecular size distribution and spectroscopic properties of aquatic humic substances. *Analytica Chimica Acta*, *337*(2), 133–149. https://doi.org/10.1016/s0003-2670(96)00412-6
Plaza, C., Pegoraro, E., Bracho, R., Celis, G., Crummer, K. G., Hutchings, J. A., et al. (2019). Direct observation of permafrost degradation and rapid soil carbon loss in tundra. *Nature Geoscience*, *12*(8), 627–631. https://doi.org/10.1038/s41561-019-0387-6

Poulin, B. A., Ryan, J. N., Nagy, K. L., Stubbins, A., Dittmar, T., Orem, W., et al. (2017). Spatial dependence of reduced sulfur in Everglades dissolved organic matter controlled by sulfate enrichment. *Environmental Science & Technology*, *51*(7), 3630–3639. https://doi.org/10.1021/acs.est.6b04142

Pugh, E. A., Olefeldt, D., Leader, S. N., Hokanson, K. J., & Devito, K. J. (2021). Characteristics of dissolved organic carbon in Boreal Lakes: High spatial and inter-annual variability controlled by landscape attributes and wet-dry periods. *Water Resources Research*, *57*(11), e2021WR030021. https://doi.org/10.1029/2021wr030021

R Core Team. (2020). *R: A language and environment for statistical computing*. R Foundation for Statistical Computing. Retrieved from https://www.R-project.org/

Šantl-Temkiv, T., Finster, K., Dittmar, T., Hansen, B. M., Thyrhaug, R., Nielsen, N. W., & Karlson, U. G. (2013). Hailstones: A window into the microbial and chemical inventory of a storm cloud. *PLoS One*, *8*(1), e53550. https://doi.org/10.1371/journal.pone.0053550

Savory, J. J., Kaiser, N. K., McKenna, A. M., Xian, F., Blakney, G. T., Rodgers, R. P., et al. (2011). Parts-per-billion Fourier transform ion cyclotron resonance mass measurement accuracy with a "walking" calibration equation. *Analytical Chemistry*, *83*(5), 1732–1736. https://doi.org/10.1021/ac102943z

Schauer, A. J., Schoenemann, S. W., & Steig, E. J. (2016). Routine high-precision analysis of triple water-isotope ratios using cavity ring-down spectroscopy. *Rapid Communications in Mass Spectrometry*, *30*(18), 2059–2069. https://doi.org/10.1002/rcm.7682

Schiff, S., Aravena, R., Mewhinney, E., Elgood, R., Warner, B., Dillon, P., & Trumbore, S. (1998). Precambrian shield wetlands: Hydrologic control of the sources and export of dissolved organic matter. *Climatic Change*, *40*(2), 167–188. https://doi.org/10.1023/a:1005496331593

Schuur, E. A., McGuire, A. D., Schädel, C., Grosse, G., Harden, J. W., Hayes, D. J., et al. (2015). Climate change and the permafrost carbon feedback. *Nature*, *520*(7546), 171–179. https://doi.org/10.1038/nature14338

Smith, L. C., Sheng, Y., MacDonald, G. M., & Hinzman, L. D. (2005). Disappearing arctic lakes. *Science*, *308*(5727), 1429. https://doi.org/10.1126/science.1108142

Sobek, S., Tranvik, L. J., & Cole, J. J. (2005). Temperature independence of carbon dioxide supersaturation in global lakes. *Global Biogeochemical Cycles*, *19*(2). https://doi.org/10.1029/2004gb002264

Solomon, C. T., Jones, S. E., Weidel, B. C., Buffam, I., Fork, M. L., Karlsson, J., et al. (2015). Ecosystem consequences of changing inputs of terrestrial dissolved organic matter to lakes: Current knowledge and future challenges. *Ecosystems*, *18*(3), 376–389. https://doi.org/10.1007/s10021-015-9848-y

Spencer, R. G., Aiken, G. R., Butler, K. D., Dornblaser, M. M., Striegl, R. G., & Hernes, P. J. (2009). Utilizing chromophoric dissolved organic matter measurements to derive export and reactivity of dissolved organic carbon exported to the Arctic ocean: A case study of the Yukon river, Alaska. *Geophysical Research Letters*, *36*(6), L06401. https://doi.org/10.1029/2008gl036831

Spencer, R. G., Aiken, G. R., Wickland, K. P., Striegl, R. G., & Hernes, P. J. (2008). Seasonal and spatial variability in dissolved organic matter quantity and composition from the Yukon River basin, Alaska. *Global Biogeochemical Cycles*, *22*(4), GB4002. https://doi.org/10.1029/2008gb003231

Spencer, R. G., Butler, K. D., & Aiken, G. R. (2012). Dissolved organic carbon and chromophoric dissolved organic matter properties of rivers in the USA. *Journal of Geophysical Research*, *117*(G3), G03001. https://doi.org/10.1029/2011jg001928

Spencer, R. G., Mann, P. J., Dittmar, T., Eglinton, T. I., McIntyre, C., Holmes, R. M., et al. (2015). Detecting the signature of permafrost thaw in Arctic rivers. *Geophysical Research Letters*, *42*(8), 2830–2835. https://doi.org/10.1002/2015gl063498

Stackpoole, S. M., Butman, D. E., Clow, D. W., Verdin, K. L., Gaglioti, B. V., Genet, H., & Striegl, R. G. (2017). Inland waters and their role in the carbon cycle of Alaska. *Ecological Applications*, *27*(5), 1403–1420. https://doi.org/10.1002/eap.1552

Stedmon, C. A., Markager, S., & Bro, R. (2003). Tracing dissolved organic matter in aquatic environments using a new approach to fluorescence spectroscopy. *Marine Chemistry*, *82*(3–4), 239–254. https://doi.org/10.1016/s0304-4203(03)00072-0

Stolpmann, L., Coch, C., Morgenstern, A., Boike, J., Fritz, M., Herzschuh, U., et al. (2021). First pan-Arctic assessment of dissolved organic carbon in lakes of the permafrost region. *Biogeosciences*, *18*(12), 3917–3936. https://doi.org/10.5194/bg-18-3917-2021

Stubbins, A., Spencer, R. G., Chen, H., Hatcher, P. G., Mopper, K., Hernes, P. J., et al. (2010). Illuminated darkness: Molecular signatures of Congo River dissolved organic matter and its photochemical alteration as revealed by ultrahigh precision mass spectrometry. *Limnology & Oceanography*, *55*(4), 1467–1477. https://doi.org/10.4319/lo.2010.55.4.1467

Tank, S. E., Lesack, L. F., Gareis, J. A., Osburn, C. L., & Hesslein, R. H. (2011). Multiple tracers demonstrate distinct sources of dissolved organic matter to lakes of the Mackenzie Delta, western Canadian Arctic. *Limnology & Oceanography*, *56*(4), 1297–1309. https://doi.org/10.4319/lo.2011.56.4.1297

Tank, S. E., Lesack, L. F., & Hesslein, R. H. (2009). Northern delta lakes as summertime CO_2 absorbers within the arctic landscape. *Ecosystems*, *12*(1), 144–157. https://doi.org/10.1007/s10021-008-9213-5

Terzer, S., Wassenaar, L. I., Araguás-Araguás, L. J., & Aggarwal, P. K. (2013). Global isoscapes for $\delta^{18}O$ and $\delta^{2}H$ in precipitation: Improved prediction using regionalized climatic regression models. *Hydrology and Earth System Sciences*, *17*(11), 4713–4728. https://doi.org/10.5194/hess-17-4713-2013

Textor, S. R., Wickland, K. P., Podgorski, D. C., Johnston, S. E., & Spencer, R. G. (2019). Dissolved organic carbon turnover in permafrost-influenced watersheds of interior Alaska: Molecular insights and the priming effect. *Frontiers of Earth Science*, *7*, 275. https://doi.org/10.3389/feart.2019.00275

Tranvik, L. J., Downing, J. A., Cotner, J. B., Loiselle, S. A., Striegl, R. G., Ballatore, T. J., et al. (2009). Lakes and reservoirs as regulators of carbon cycling and climate. *Limnology & Oceanography*, *54*(6), 2298–2314. https://doi.org/10.4319/lo.2009.54.6_part_2.2298

Verpoorter, C., Kutser, T., Seekell, D. A., & Tranvik, L. J. (2014). A global inventory of lakes based on high-resolution satellite imagery. *Geophysical Research Letters*, *41*(18), 6396–6402. https://doi.org/10.1002/2014gl060641

Vonk, J. E., Tank, S. E., Mann, P. J., Spencer, R. G., Treat, C. C., Striegl, R. G., et al. (2015). Biodegradability of dissolved organic carbon in permafrost soils and aquatic systems: A meta-analysis. *Biogeosciences*, *12*(23), 6915–6930. https://doi.org/10.5194/bg-12-6915-2015

Walter Anthony, K., Schneider von Deimling, T., Nitze, I., Frolking, S., Emond, A., Daanen, R., et al. (2018). 21st-century modeled permafrost carbon emissions accelerated by abrupt thaw beneath lakes. *Nature Communications*, *9*(1), 1–11. https://doi.org/10.1038/s41467-018-05738-9

Walvoord, M. A., Voss, C. I., & Wellman, T. P. (2012). Influence of permafrost distribution on groundwater flow in the context of climate-driven permafrost thaw: Example from Yukon Flats Basin, Alaska, United States. *Water Resources Research*, *48*(7), W07524. https://doi.org/10.1029/2011wr011595

Weishaar, J. L., Aiken, G. R., Bergamaschi, B. A., Fram, M. S., Fujii, R., & Mopper, K. (2003). Evaluation of specific ultraviolet absorbance as an indicator of the chemical composition and reactivity of dissolved organic carbon. *Environmental Science & Technology*, *37*(20), 4702–4708. https://doi.org/10.1021/es030360x

Wickham, H. (2016). *ggplot2: Elegant graphics for data analysis*. Springer.

Wickland, K. P., Aiken, G. R., Butler, K., Dornblaser, M. M., Spencer, R. G. M., & Striegl, R. G. (2012). Biodegradability of dissolved organic carbon in the Yukon River and its tributaries: Seasonality and importance of inorganic nitrogen. *Global Biogeochemical Cycles*, *26*(4), GB004342. https://doi.org/10.1029/2012gb004342

Wickland, K. P., Jorgenson, M. T., Koch, J. C., Kanevskiy, M., & Striegl, R. G. (2020). Carbon dioxide and methane flux in a dynamic Arctic tundra landscape: Decadal-scale impacts of ice wedge degradation and stabilization. *Geophysical Research Letters*, *47*(22), e2020GL089894. https://doi.org/10.1029/2020gl089894

Wickland, K. P., Neff, J. C., & Aiken, G. R. (2007). Dissolved organic carbon in Alaskan boreal forest: Sources, chemical characteristics, and biodegradability. *Ecosystems*, *10*(8), 1323–1340. https://doi.org/10.1007/s10021-007-9101-4

Wologo, E., Shakil, S., Zolkos, S., Textor, S., Ewing, S., Klassen, J., et al. (2021). Stream dissolved organic matter in permafrost regions shows surprising compositional similarities but negative priming and nutrient effects. *Global Biogeochemical Cycles*, *35*(1), e2020GB006719. https://doi.org/10.1029/2020gb006719

Zherebker, A., Kim, S., Schmitt-Kopplin, P., Spencer, R. G., Lechtenfeld, O., Podgorski, D. C., et al. (2020). Interlaboratory comparison of humic substances compositional space as measured by Fourier transform ion cyclotron resonance mass spectrometry (IUPAC Technical Report). *Pure and Applied Chemistry*, *1*(9), 1447–1467. https://doi.org/10.1515/pac-2019-0809

References From the Supporting Information

Brown, J., Ferrians, Jr. O. J., Heginbottom, J. A., & Melnikov, E. S. (1997). *Circum-arctic map of permafrost and ground ice conditions*. National Snow and Ice Data Center. https://doi.org/10.7265/skbg-kf16

Elder, C. D., Xu, X., Walker, J., Schnell, J. L., Hinkel, K. M., Townsend-Small, A., et al. (2018). Greenhouse gas emissions from diverse Arctic Alaskan lakes are dominated by young carbon. *Nature Climate Change*, *8*(2), 166–171. https://doi.org/10.1038/s41558-017-0066-9

Hinkel, K. M., Eisner, W. R., Bockheim, J. G., Nelson, F. E., Peterson, K. M., & Dai, X. (2003). Spatial extent, age, and carbon stocks in drained thaw lake basins on the Barrow Peninsula. *Alaska. Arctic, Antarctic, and Alpine Research*, *35*(3), 291–300. https://doi.org/10.1657/1523-0430(2003)035[0291:SEAACS]2.0.CO;2

Obu, J., Westermann, S., Barboux, C., Bartsch, A., Delaloye, R., Grosse, G., et al. (2021). *ESA permafrost climate change initiative (permafrost_cci): Permafrost extent for the Northern Hemisphere, v3. 0'*. CEDA. Retrieved from https://catalogue.ceda.ac.uk/uuid/6e2091cb0c8b4106921b63cd5357c97c

Peters, D. L., Prowse, T. D., Marsh, P., Lafleur, P. M., & Buttle, J. M. (2006). Persistence of water within perched basins of the Peace-Athabasca delta, northern Canada. In *Wetlands ecology and management* (Vol. *14*, pp. 221–243).